Πανεπιστήμιο Κρήτης

Σχολή Θετικών Επιστημών

Τμήμα Βιολογίας

Ίδρυμα Τεχνολογίας και Έρευνας (ΙΤΕ)

Ινστιτούτο Μοριακής Βιολογίας και Βιοτεχνολογίας (IMBB)

Εργαστήριο Μοριακής Εντομολογίας

Πρόγραμμα Μεταπτυχιακών Σπουδών Μοριακής Βιολογίας και Βιοϊατρικής

Μεταπτυχιακή διπλωματική εργασία

Βιοτεχνολογικές προσεγγίσεις για την ανακάλυψη εντομοκτόνων

Μάνθα Λαμπρούση

Επιβλέπων: Ιωάννης Βόντας, Καθηγητής

Τριμελής επιτροπή:

Ιωάννης Βόντας, Καθηγητής

Χρήστος Δελιδάκης, Καθηγητής

Παναγιώτης Σαρρής, Αναπληρωτής Καθηγητής

Ηράκλειο, Οκτώβριος 2019

University of Crete

Faculty of Sciences

School of Biology

Foundation of Research and Technology- Hellas (FORTH)

Institute of Molecular Biology and Biotechnology (IMBB)

Laboratory of Molecular Entomology

Joint Graduate program in Molecular Biology and Biomedicine (JPG- MBB)

Master thesis

Biotechnology- based approaches for insecticide discovery

Mantha Lamprousi

Supervisor: John Vontas, Professor

Committee:

John Vontas, Professor

Christos Delidakis, Professor

Panagiotis Sarris, Associate Professor

Heraklion, October 2019

Abstract

Insecticides resistance is a constantly increasing problem in recent years, as crops and human health are threatened by agricultural pests and disease vectors, respectively. For this reason, it is imperative to find new insecticide targets and also to investigate the role of several mutations in insecticide resistance through functional validation. The midgut of insects is the most important tissue involved in penetration of insecticides and their entrance to the hemocoel in order to cause their toxic effects in specific tissues where their targets lie.

Several Lepidopteran species like *Helicoverpa armigera* are major agricultural pests and they can easily develop resistance. Thus, the investigation of lepidopteran midgut properties is essential. We tried to established a primary midgut cell line from *H. armigera* in order to investigate the properties of the different midgut cell types (intestinal stem cells, enterocytes, enteroendocrine cells and Goblet cells), with a major focus on intestinal stem cell properties because of their ability to give rise to all the different midgut cell types and to enterocyte properties due to the role of apical-basolateral polarization and the existence of microvilli in absorption, penetration and diffusion of different compounds,.

We also investigated certain properties (transfectability and spheroids formation) of an already established lepidopteran midgut cell line from *Helicoverpa zea* (RP-HzGUT- AW1), a close relative of *H. armigera*. Transcriptomics analysis was performed for these cells in order to characterize their expression profile. One major question regarding these cells was if the spheroids formed develop smooth septate junctions (sSJs) as expected in midgut epithelia. This was examined by comparing the levels of expression of various genes involved in sSJs formation, in particular three main regulators: Mesh, tetraspanin- 2A (Tsp2A) and snakeskin (Ssk). While various other markers were identified from transcriptomics for characterization of *H. zea* midgut cell line, the expression levels of sSJs markers were not significantly altered.

Regarding functional validation of mutations possibly associated with target-site insecticide resistance, a mutation first identified in *glutamate gated chloride 3 subunit* (*GluCl*) of the spider mite *Tetranychus urticae* and associated with resistance to abamectin was investigated. This mutation (I310T) was introduced to the *Drosophila melanogaster GluCl*, with the CRISPR/ Cas9 genome editing tool, in order to functionally validate its contribution to abamectin resistance.

Finally, in order to facilitate functional characterization of certain cytochrome P450 momoxygenases, a class of enzymes that among other roles, contribute also, to xenobiotic detoxification in insects, we performed, functional expression of three P450s from *Apis mellifera* using the baculovirus expression system. For this purpose, we used different baculovirus combinations and co-infected Sf9 cells in order to co- express each honeybee P450 with P450 reductase (CPR) to generate a functional complex. We performed Western analysis to detect both P450 and CPR in membrane extracts of infected cells and also performed with CO spectrum and CPR activity assays that indicated that the membrane extracts contain are functional complexes that can be used for downstream assays.

Περίληψη

Η ανθεκτικότητα στα εντομοκτόνα αποτελεί ένα διαρκώς αυξανόμενο πρόβλημα τα τελευταία χρόνια, καθώς οι καλλιέργειες και η ανθρώπινη υγεία απειλούνται από γεωργικά παράσιτα και φορείς ασθενειών, αντίστοιχα. Για το λόγο αυτό είναι επιτακτική η εξεύρεση νέων στόχων εντομοκτόνων και επίσης η διερεύνηση του ρόλου διαφόρων μεταλλάξεων στην αντοχή εντομοκτόνων μέσω λειτουργικής επικύρωσης. Το μεσαίο έντερο είναι ο σημαντικότερος ιστός που εμπλέκεται στη διείσδυση των εντομοκτόνων και την είσοδό τους στην αιμόλεμφο για να προκαλέσει τις τοξικές τους επιδράσεις σε συγκεκριμένους ιστούς όπου βρίσκονται οι στόχοι τους.

Αρκετά είδη λεπιδοπτέρων, όπως το *Helicoverpa armigera,* αποτελούν τα σημαντικότερα γεωργικά παράσιτα και μπορούν εύκολα να αναπτύξουν αντίσταση. Έτσι, η διερεύνηση των ιδιοτήτων του midgut των λεπιδοπτέρων είναι απαραίτητη. Προσπαθήσαμε να δημιουργήσουμε μια πρωτογενή κυτταρική σειρά midgut από το *H. Armigera* προκειμένου να διερευνήσουμε τις ιδιότητες των διαφορετικών εντερικών κυτταρικών τύπων (intestinal stem cells, enterocytes, enteroendocrine cells και Goblet cells), με ιδιαίτερη έμφαση στις ιδιότητες των εντερικών βλαστικών κυττάρων (intestinal stem cells) εξαιτίας της ικανότητά τους να γεννούν όλους τους διαφορετικούς τύπους κυττάρων του midgut και στις ιδιότητες των εντεροκυττάρων (enterocytes) εξαιτίας του ρόλου της βασικοπολικής πόλωσης και της ύπαρξης μικρολαχνών στην απορρόφηση, τη διείσδυση και τη διάχυση διαφορετικών ενώσεων.

Διερευνήσαμε επίσης ορισμένες ιδιότητες (transfectability και spheroids formation) μίας ήδη καθιερωμένης κυτταρικής σειράς από midgut λεπιδόπτερου, από το *Helicoverpa zea* (RP-HzGUT-AW1), στενός συγγενής του *H. Armigera*. Διεξήχθη transcriptomics analysis για αυτά τα κύτταρα προκειμένου να χαρακτηριστεί το προφίλ έκφρασής τους. Μία σημαντική ερώτηση σχετικά με αυτά τα κύτταρα ήταν αν τα σφαιροειδή σχηματίζουν smooth septate junctions (sSJs) όπως αναμένεται στο επιθήλιο του midgut. Αυτό εξετάστηκε με τη σύγκριση των επιπέδων έκφρασης των διαφόρων γονιδίων που εμπλέκονται στο σχηματισμό sSJs, ιδιαίτερα τριών κύριων ρυθμιστών: *Mesh, tetraspanin-2A (Tsp2A)* και *snakeskin (Ssk*). Αν και διάφοροι άλλοι δείκτες ταυτοποιήθηκαν από τα transcrisptomics για τον χαρακτηρισμό της κυτταρικής σειράς από το midgut του *H. Zea*, τα επίπεδα έκφρασης των δεικτών sSJs δεν μεταβλήθηκαν σημαντικά.

Όσον αφορά τη λειτουργική αξιολόγηση των μεταλλάξεων που πιθανώς σχετίζονται με την target- site ανθεκτικότητα εντομοκτόνων, διερευνήθηκε μια μετάλλαξη που εντοπίστηκε πρώτα στην υπομονάδα χλωριούχου γλουταμινικού 3 (GluC1) του *Tetranychus urticae* και συσχετίστηκε με αντίσταση στο abamectin. Αυτή η μετάλλαξη (I310T) εισήχθη στο *GluCI* γονίδιο της *Drosophila melanogaster*, με το εργαλείο επεξεργασίας γονιδιώματος CRISPR / Cas9, προκειμένου να αξιολογηθεί λειτουργικά η συμβολή του στην αντίσταση στο abamectin.

Τέλος, προκειμένου να διευκολυνθεί ο λειτουργικός χαρακτηρισμός ορισμένων κυτοχρωμικών P450 μονοξυγενασών, μία τάξη ενζύμων που μεταξύ των άλλων ρόλων τους συνεισφέρουν επίσης και στην ξενοβιοτική αποτοξίνωση στα έντομα, πραγματοποιήθηκε η λειτουργική έκφραση τριών P450s από το *Apis mellifera* χρησιμοποιώντας το σύστημα έκφρασης baculovirus. Για το σκοπό αυτό, χρησιμοποιήσαμε διαφορετικούς συνδυασμούς baculovirus και συν-μολυσμένα Sf9

κύτταρα προκειμένου να συν-εκφράσουμε κάθε P450 μέλισσας με P450 αναγωγάση (CPR) για να δημιουργήσουμε ένα λειτουργικό σύμπλεγμα. Διεξήγαμε ανάλυση Western για να ανιχνεύσουμε και τις P450s και τη CPR σε εκχυλίσματα μεμβρανών μολυσμένων κυττάρων και επίσης διεξήχθησαν δοκιμασίες CO φάσματος και CPR δραστηριότητας που έδειξαν ότι τα εκχυλίσματα μεμβράνης περιέχουν λειτουργικά σύμπλοκα που μπορούν να χρησιμοποιηθούν για παρακάτω αναλύσεις.

Ευχαριστίες

Η παρούσα μεταπτυχιακή διπλωματική εργασία εκπονήθηκε στο εργαστήριο Μοριακής Εντομολογίας του Ινστιτούτου Μοριακής Βιολογίας και Βιοτεχνολογίας (IMBB) που ανήκει στο Ίδρυμα Τεχνολογικών Ερευνών (ΙΤΕ) κατά το ακαδημαϊκό έτος 2018- 2019 υπό την επίβλεψη του κ. Δρ Ιωάννη Βόντα, Καθηγητή του Γεωπονικού Πανεπιστημίου Αθηνών και ερευνητή στο IMBB. Αυτή η διπλωματική εργασία δε θα είχε πραγματοποιηθεί και ολοκληρωθεί χωρίς τη συμβολή πολλών ανθρώπων τους οποίου θα ήθελα να ευχαριστήσω από την καρδιά μου για την κάθε είδους προσφορά.

Αρχικά θα ήθελα να ευχαριστήσω θερμά τον επιβλέποντα καθηγητή μου κ. Ιωάννη Βόντα, ο οποίος με εμπιστεύτηκε και μου έδωσε την ευκαιρία να εκπονήσω τη διπλωματική μου εργασία στο συγκεκριμένο εργαστήριο πάνω σε θέματα που μου εξάπτουν την περιέργεια. Θα ήθελα να την ευχαριστήσω για την υποστήριξη, την καθοδήγηση που μου έδωσε αλλά και την ευκαιρία να παρευρεθώ σε συνέδριο, summer school, σε meetings με στενούς συνεργάτες, αλλά και να ασχοληθώ με πολλά διαφορετικά projects. Θα ήθελα επίσης να ευχαριστήσω τον κ. Ιωάννη Βόντα, τον καθηγητή κ. Χρήστο Δελιδάκη και τον αναπληρωτή καθηγητή κ. Παναγιώτη Σαρρή για την επίβλεψη, τις συμβουλές και τις διορθώσεις των qualifying examinations και της παρούσας διπλωματικής εργασίας.

Ένα μεγάλο ευχαριστώ οφείλω κ. Δρ Βασίλειο Δουρή, Επίκουρο Καθηγητή, πλέον, του Πανεπιστημίου Ιωαννίνων για την πνευματική καθοδήγηση και τις συμβουλές, καθ' όλη την ακαδημαϊκή χρονιά. Επίσης θα ήθελα να τον ευχαριστήσω για τις διορθώσεις στην παρούσα πτυχιακή εργασία. Χάρη σε εκείνον εξέλιξα τον επιστημονικό τρόπο σκέψης μου και την συμπεριφορά μου μέσα στο εργαστήριο. Εκείνος μου δίδαξε τη μέθοδο CRISPR/ Cas9. Χάρη στη δική του παρότρυνση έμαθα να έχω υπομονή και επιμονή για τα πειράματα και να αντιμετωπίζω με ψυχραιμία και κριτική τυχόν πειραματικά προβλήματα.

Εν συνεχεία θα ήθελα να ευχαριστήσω την κ. Δρ Έλενα Βοργιά διότι ήταν εκείνη που με μύησε στις κυτταρικές σειρές και με δίδαξε τεχνικές που σχετίζονται μ' αυτές, όπως και τον κ. Δρ Shane Denecke καθώς με βοήθησε με την ανάλυση των transcriptomics data και πρόσφερε απλόχερα την επιστημονική κριτική του σκέψη όποτε τη ζητούσα. Επιπλέον τις τεχνικούς των εργαστηρίων κ. Σοφία Καφώρου και κ. Δήμητρα Τσακιρέλη τις τεχνικές που μου δίδαξαν και γιατί είχαν πάντα μια λύση για τα πειραματικά προβλήματα. Την κ. Τσακιρέλη θα ήθελα να την ευχαριστήσω καθώς έκανε όλα τα βιοχημικά πειράματα στο project με τις P450s.

Ακόμα θα ήθελα να εκφράσω τις θερμές ευχαριστίες μου στους υποψήφιους διδάκτορες κ. Γιώργο Σαμαντσίδη και κ. Ραφαέλα Παντελέρη καθώς ήταν αυτοί που με δίδαξαν όσα ξέρω για το χειρισμό της *Drosophila melanogaster*. Τον κ. Σαμαντσίδη θα ήθελα να τον ευχαριστήσω επίσης για τις συμβουλές του και την καθοδήγηση στο cloning. Επιπλέον ευχαριστώ την υποψήφια διδάκτορα κ. Κυριακή- Μαρία Παπαποστόλου και τη μεταπτυχιακή φοιτήτρια Ευαγγελία Σκούφα για τη βοήθεια και τα αποτελέσματά τους στο project με τον τετράνυχο. Ευχαριστώ τον κ. Δρ Άρη Ηλία για τη φροντίδα των ζώων που χρησιμοποιούσαμε για τα primary και για την καθοδήγησή του στα sequencing και την κ. Δρ Μαρία Ρήγα για την κατασκευή των BACmids στο project με τις P450s. Επιπρόσθετα ευχαριστώ τους τεχνικούς του IMBB κ. Ιωάννη Λειβαδάρα για τις ενέσεις στη *Drosophila* και τον κ. Γεώργιο Βρέντζο για τη συντήρηση του insect cell culture room. Επιπρόσθετα, θα ήθελα να ευχαριστήσω

όλα τα μέλη του εργαστηρίου για τη βοήθεια, τη στήριξη, τις συμβουλές που πρόσφεραν και το ευχάριστο κλίμα εργασίας που δημιούργησαν και διατήρησαν καθ' όλη τη χρονιά.

Κλείνοντας οφείλω ένα τεράστιο ευχαριστώ στους γονείς μου που με στηρίζουν όλα αυτά τα χρόνια οικονομικά και ηθικά καθώς και την υπομονή που δείχνουν αλλά και τους φίλους και συμφοιτητές μου από το μεταπτυχιακό πρόγραμμα που έκαναν αυτά τα 2 χρόνια, παρά τις όποιες δυσκολίες, να είναι διασκεδαστικά και ανεκτίμητα.

Contents

1. Introduction

1.1 The problem of insecticide resistance- Resistance mechanisms

The continued growth of global human population has raised the world demands for food. However, crops are the target of several pests which have in recent years developed increased levels of pesticide resistance (e.g. the spider mite *Tetranychus urticae* and the lepidopteran insect *Helicoverpa armigera*). Furthermore, resistance against insecticides has evolved in several insect species which are disease vectors (e.g. the mosquito *Anopheles gambiae*). The term "insecticide resistance" refers to the heritable shift in the tolerance of the pest population expressed in natural or chemical compounds' repeated failure to achieve the desired level of control (Insecticide Resistance Action Committee, https://www.irac-online.org/). Historically, resistance started developing very soon following the widespread application of insecticides; one of the first cases of resistance was discovered back in 1947, in the mosquito species *Aedes tritaeniorhynchus* and *Aedes sollicitans* against DDT, after only 1 year of DDT spraying (Brown, Ruzo *et al*. 1986). Moreover, the two-spotted spider mite (*Tetranychus urticae*) was the first glasshouse pest to develop resistance back in 1949 (Chattopadhyay, Banerjee *et al*. 2017). Since then, every new insecticide entry has been accompanied by resistance development because of the genetics of heritable resistance and the intensive repeated application of pesticides (Insecticide Resistance Action Committee, https://www.irac-online.org/).

The insecticide's selection pressure enables some initially very rare, naturally occurring due to the standing genetic variation of populations, pre- adapted insects with resistance alleles to survive and pass on their offspring the resistance trait. While continuing to administer insecticides with the same mode of action (MoA), selection of resistant individuals continues to increase the proportion of resistant insects in the population, while the insecticide removes susceptible individuals. Resistant insects outnumber susceptible ones under permanent selection pressure and the insecticide is no longer effective. How fast resistance will develop depends on a number of factors including the rate of reproduction of insects, the range of migration and hosting of pests, the availability of susceptible populations nearby, the persistence and specificity of the crop protection and the rate, timing and number of applications (Insecticide Resistance Action Committee, https://www.irac-online.org/).

The majority of commercially available insecticides have a mode of action targeting the nervous system, while some act against growth regulation and energy metabolism. Except DDT, which is the first and most well-known neuronal insecticide, there are more classes like organophosphates, pyrethroids and neonicotinoids (Casida and Durkin 2013). Neuronal synthetic insecticides are so popular for many reasons. One of these is their quick action. Moreover, there are lots of vulnerable target sites that can ultimately prove lethal even with a minor disturbance. A lipoidal sheath provides protection to insect nerves from ionized toxicants but not from lipophilic insecticides. Finally, weak nerve detoxification processes have long- term effects of toxicants (Casida and Durkin, 2013).

These insecticides have several different targets in nervous system. One of them is acetylcholinesterase, which is responsible for hydrolysis of acetylcholine at synaptic regions of cholinergic nerve endings. Its inhibitors act at cholinergic receptors where acetylcholine is accumulated and cause their extravagant stimulation. Such inhibitors are organophosphates and methylcarbamates. Another target is nicotinic acetylcholine receptor which is the receptor for the principal excitatory transmitter for neurotransmission, acetylcholine, in the insect central nervous system. Imidacloprid

acts as an antagonist of acetylcholine that binds permanent to acetylcholine receptors and causes hyperexcitation and insect paralysis. Fipronil and other insecticides block gamma-aminobutyric acid (GABA) induced signals and Cl^- efflux, since GABA, the principal inhibitory neurotransmitter acts as the antagonist for opening the pentameric transmembrane Cl^- channel which is another target. Sodium channel is also susceptible in some insecticides such as pyrethrins and DDT. These insecticides induce excitation by binding to resting or inactivated channels and cause repetitive activity due to a slowly activating Na^+ current. Another action of these insecticides is that they keep Na^+ channels into permanent open states. Furthermore, octopamine receptors and ryanodine receptors constitute insecticide targets as well (see review by Casida and Durkin, 2013).

The molecular mechanisms responsible for insecticide resistance can be classified in four different types: **metabolic resistance**, **target- site resistance**, **penetration resistance** and **behavioral resistance**. Target site resistance is caused by point mutations in target genes which are followed by changes in amino acids and protein structure. These changes do not allow the insecticide molecules to bind or interact with their target sites. Metabolic resistance defines an insect's ability to increase detoxification efficiency, such as enzyme overexpression or raised detoxification enzyme association with insecticide molecules. Gene families which encode detoxification enzymes responsible for metabolic insecticide resistance are the multifunction oxidases (family of cytochrome P450 monooxygenases), glutathione- S-transferases, and esterases (Ffrench- Constant, 2013). In addition, penetration or cuticle resistance is characterized by a slower penetration of insecticides into the cuticle of insects (e.g. mosquitoes) and in some cases can be also associated with metabolic resistance (Balabanidou *et al.,* 2016). Finally, behavioral resistance is defined as the insecticides' recognition by the insect (known for organochlorines, organophosphates, carbamates and pyrethroids) and its subsequent avoidance behavior (Oppold and Mueller, 2017).

1.2 New insecticide targets / development of assays as screening tools

1.2.1 Insect alimentary canal (gut)

The relatively limited number of available molecular targets for insecticides, along with the emergence of resistance and the regulatory limitations imposed by public health and environmental concerns, have generated an urging need to identify new potential insecticide targets/modes of action as well as develop novel screening tools for the validation of new chemistries. Significant research effort is directed towards these goals.

The majority of insecticides are oral and delivered to the insect target via ingestion. Then, they arrive at the alimentary canal (gut), they penetrate it and are transferred through the hemocoel to the tissues (nerve, muscle, etc.) which they specifically target (see review by Denecke, Swevers *et al.* 2018). Thus, the critical step is that the insecticides achieve gut penetration in order to manifest their lethal action. Efforts have been made for discovering insecticide targets expressed within the gut. However, only toxins from *Bacillus thurigiensis* and *Bacillus sphaericus* have been proved to have this action so far (Denecke *et al.,* 2018).

The gut is a hollow tube beginning from mouth and ending to anus. In most insects it is separated in three defined parts: the foregut (anterior part), the midgut (middle part) and the hindgut (posterior part). The foregut and hindgut are derived from ectoderm and are surrounded by a thin cuticular layer. The morphology of these two parts varies significantly between insect species, but two parts which they share are a distinguishable crop for food storage in the foregut and a rectum for holding waste in

the hindgut. The midgut is derived from the endoderm and it is constituted by a single cell thick "brush border" epithelium and surrounded (at the apical side) by an acellular, chitinous structure, known as peritrophic matrix. The midgut is considered as the part of gut where oral insecticide penetration occurs (Denecke *et al.,* 2018).

The basolateral surface of the midgut is in contact with hemolymph, a lattice of muscle cells and an acellular basal lamina consisting of collagen, laminin and other proteins. Furthermore, sometimes the midgut can be further divided into anterior, middle and posterior regions, as in lepidopteran larvae. The lepidopteran midgut epithelium is consisted of four distinct cell types: the intestinal stem cells (ISCs), the enteroendocrine cells (EEs), the Goblet cells (GCs) and the enterocytes or columnar cells (ECs). Intestinal stem cells are small, diploid and located near the basolateral membrane without communication with the lumen (Cermenati *et al*., 2007). Their function is to give rise to other cell types. Enteroendocrine cells are bigger, and they communicate with the gut lumen. They produce enteropteprides (also called neuropeptides) which are responsible for communication between the cells. Goblet cells, (which have different function from the mammalian gut cells with the same name), seem to have a role in ion transport and gut alkalization. Goblet cells are a characteristic lepidopteran midgut cell type, presumably related with the elevated alcalic pH found in lepidopteran midgets, whereas they do not exist in *Drosophila melanogaster* midgut (Denecke *et al.*, 2018).

The most abundant and characteristic cell type of the lepidopteran midgut is the enterocytes (EC), which are distinct from the rest of the cell types because of their extensive apical microvilli. ECs seem to have the most significant role in insecticide penetration through the midgut. They are connected to each other by smooth septate junctions (SSJs). They seem to have multiple functions such as ion transport, absorption of nutrients and secretion of digestive enzymes (e.g. trypsins, amylases) into the gut lumen (Denecke *et al.,* 2018).

As previously mentioned, insecticides need to penetrate the midgut epithelium in order to enter the hemolymph and reach the target tissue. Different compounds may require different ways of penetration: transcellular diffusion, paracellular diffusion, via transporter proteins for small molecules and endocytosis and paracellular diffusion for proteins and peptides. In particular, paracelluar diffusion includes the route of small molecules around the cell for reaching the hemolymph. Regarding this route, small molecules should go through the septate junctions (SJs). SJs connect epithelial cells and are analogous (though not homologous) to the intestinal vertebrate tight junctions. The SJs can be distinguished in pleated type junctions (pSJs) in ectodermal epithelial tissues and smooth septate junctions (sSJs) in endodermal tissues like the midgut. The specific protein components of these junctions snakeskin (Ssk) and Mesh have been identified in the silkworm midgut (Izumi, Yanagihashi *et al*. 2012, Yanagihashi, Usui *et al*. 2012) and together with with tetraspanin 2A (Tsp2A) it has been shown that they form a complex in *Drosophila*, where they are key components for sSJs constitution and gut barrier function (Furuse and Izumi 2017).

1.2.2 Cell based assays and 3D cultures

In order to discover new strategies for pest control related to midgut penetration, it is important to study first the properties of different midgut cell types and the different penetration ways of the midgut tissue. A really useful tool that can potentially be developed towards this purpose is the use of insect cell lines for the generation of cell-based assays and 3D cultures (spheroids, organoids), if this is feasible. A common assay which is usually used as an assay to test the perameability and the absorption of different pharmaceutical drug compounds in mammalian cell systems is the Caco- 2 permeability assay (Press and Di Grandi 2008). Caco-2 cell line is a continuous line of heterogenous human epithelial colorectal adenocarcinoma (Press and Di Grandi, 2008), which is used to test different compounds' permeability, mainly in drug discovery pipelines (Sun, Chow *et al.* 2008). These cells generate a confluent epithelial cell monolayer which imitates columnar and polarized cells that form microvilli on the apical membrane and tight junctions between neighboring cells, after being cultured in a plate or transwell (Sun *et al.,* 2008). This assay is usually used for passively absorbed drugs. Caco-2 cells express diverse transporters, enzymes and nuclear receptors enabling various applications of Caco- 2 cell monolayer such as drug permeability screening, identifying transport mechanisms (paracellular pathways, active uptake and carrier- mediated efflux) and gene expression upon exposure to drugs or drug- like compounds (Sun *et al.,* 2008).

Conventional 2D culture-based assays are used as a first step, before animal testing, for screening compounds with possible pharmaceutical role during drug discovery (Edmondson, Broglie *et al.* 2014). Most of the compounds fail during clinical trials, so it is a great need to create tools which will simulate the tissue microenvironment. Hence, in recent years the use of 3D cultures in drug screening has increased. It is thought that 3D cultures are a more representative tool of tissue microenvironment compared to 2D cultures. 3D and 2D cultures have different morphological and physiological characteristics, with 3D cultures tending to be more similar to the *in vivo* behavior. 3D cell cultures have been used in drug discovery, cancer biology, stem cell biology, tissue engineering, etc. because they provide an important tool for studying cellular responses (Edmondson *et al.,* 2014).

In mammalian cell cultures, 2D and 3D cultures seem to have many differences. Morphologically, 2D cells are characterized by a flat monolayer, whereas 3D cells have a natural shape in spheroid or aggregate structure. 2D cell cultures are exposed similarly to growth factors, nutrients and other compounds that are distributed in growth medium. In contrast, only the outer layer of a spheroid is exposed to compounds, which may not penetrate the spheroid entirely and enter the cells close to the core. The gene and protein expression of spheroids seem to be more similar with *in vivo* models in comparison to 2D cultures. Finally, spheroids appear to be a more representative system for predicting the cell responses to a compound, since they are more resistant to treatments that 2D cells. Thus, 3D cell cultures are apparently better models than 2D cell cultures because of interactions among the cells and their architecture which is reminiscent of *in vivo* tissues (Edmondson *et al.*, 2014).

In principle, insect cell cultures are quite different from mammalian in the sense that they are not derived from tumors, but their generation is spontaneous, and is believed to be reliant on the proliferation of stem cells that fail to undergo full differentiation (Lynn 1996; Smagghe *et al*., 2009). Most available insect cell lines consist of cells that

are not attached and grow in suspension rather than 2D layer. Thus, no “Caco-2 type” or 3D based assay is currently available, and the need to further investigate this field is evident.

1.2.3 Smooth septate junctions (sSJs) and midgut cell type markers

Concerning all the tools available in mammalian cells, a major question is if similar tools are applicable to insect cells. Using tools similar to the Caco-2 assay in insect cells would generate the ability to study paracellular transport through the investigation of sSJs (see par. 1.2.1). Furthermore, the investigation of cultured midgut cell properties may provide insight towards the development of other cell-based assays. As there are no available sources in the literature about lepidopteran midgut cell specific markers, studies in *Drosophila melanogaster* midgut can pave the way. Hung *et al*. (2018) have managed to discover novel molecular markers, further characterize gene expression and cell types in the adult *Drosophila* midgut by performing single- cell RNA sequencing. Different signaling pathways participate in cell proliferation, regeneration and differentiation in the *Drosophila* midgut. Notch pathway is implicated in ISCs differentiation by expression of the Notch signal (Micchelli and Perrimon, 2006) whereas EGFR, JAK/ STAT and Hippo pathways are implicated in intestinal stem cells growth and proliferation. Studies of dissociated Lepidopteran midguts found that cell death caused by *Bacillus thuringiensis* endotoxin stimulated the division of a population of cells that were probably ISCs (Loeb *et al*., 2001). Loss of damaged ECs stimulates ISC division, also, in *D. melanograster* (Shaw *et al.*, 2010) and activates signaling pathways. Damaged or stressed ECs produce the *Unpaired* cytokines (*Upd*, *Upd2*, and *Upd3*) which trigger Jak/Stat signaling in ISCs and enteroblasts (EBs), promoting their division and differentiation, respectively, and thereby driving renewal of the gut epithelium. (Jiang *et al.*,2009). Hippo pathway targets are, also, induced by stresses such as bacterial infection, suggesting that the Hippo pathway functions as a sensor of cellular stress in the differentiated cells of the midgut and through Yki, the pro-growth transcription factor target of the Hippo pathway, is a mediator of the regenerative response in the *Drosophila* midgut (Shaw *et al.,* 2010). Furthermore, response to damage or stress in the intestinal (midgut) epithelium of adult *Drosophila*, leads to the activation of EGFR signaling which promotes ISC division and midgut epithelium regeneration, thereby maintaining tissue homeostasis. In addition, ISC proliferation induced by Jak/Stat signaling is dependent upon EGFR signaling (Jiang *et al.,* 2011). EBs, which is an ISCs progeny, are characterized by the *Su(H)- lacZ* expression, a Notch activity reporter and *escargot*, a SNAIL family transcription factor. *Escargot* is a critical stem cell determinant that maintains stemness by repressing differentiation-promoting factors, such as Pdm1 (Korzelius *et al*., 2014).

On the other hand, enterocytes (ECs) are defined by *Myosin31DF* (*Myo1A*) and *nubbin* (or *pdm1*) expression. Marker genes for entroendocrine cells are *prospero* and *Piezo,* which encodes a sensor cation channel for mechanical tension. In *Drosphila* midgut, nine hormones are secreted by EEs which are located in different midgut compartments. These hormones are: allatostatins (AstA, AstB/ MIP, AstC), tachykinin, neuropeptide F (NPF), DH31, CCHa1, CCHa2 and orchokinin B. Regarding Goblet

cells (GCs), which do not exist in *Drosophila* midgut, genes which encode ATPase subunit genes (Klein, 1992), can be used as markers for this specific cell type.

1.3 Target-site mutations and CRISPR validation in *Drosophila*

1.3.1 Target site mutations in *Tetranychus urticae* Glutamate gated Chloride channel (GluCl)

Tetranychus urticae is an acari and is considered one of the most important agricultural pests. It is extremely plant polyphagous (Dermauw, Ilias *et al*. 2012). Glutamate gated chloride channels (GluCls) belong to gene superfamily of cys- loop ligand- gated ion channel (cysLGIC) of neurotransmitter receptors. Characteristic morphological feature of genes that belong to this family is that each receptor has five subunits with transmembrane and extracellular domains which generate an ion pore and binding sites where a neurotransmitter tethers. *T. urticae* has five paralogous *GluCl* genes, whereas most of the insects (e.g *Drosophila melanogaster, Tribolium castaneum,* etc.) have only one gene copy. All *Tetranychus* genes have 68.4- 76.1% similarity with *D. melanogaster* orthologue (Dermauw *et al*., 2012).

cysLGIC constitutes also targets for many known insecticides and acaricides (Kwon *et al*., 2010; Dermauw *et al*., 2012). Avermectin tethers to GluCls and occurs to irreversible opening of the channels, influx of Cl^-, hyperpolarization and paralysis (Mounsey, Dent *et al*. 2007). Abamectin, which belongs to avermectins, is a macrocyclic lactone compound, has been isolated from *Streptomyces avermitilis* and binds also to GluCls (Kwon, Yoon *et al.* 2010). Many insecticide resistant mutations have been reported in *T. urticae GluCl* genes (Mermans, Dermauw *et al.* 2017).

1.3.2. Discovery of the mutation (I310T) in *glutamate chloride channel (GluCl)* gene of *Tetranychus urticae*

A novel mutation was detected at glutamate chloride channel 3 (GluCl3) gene in Trizinia field population of *Tetranychus urticae* (Papapostolou and Vontas, unpublished data)**.** The mutation found in Trizinia population is a substitution from Ile (ATT) to Thr (ACC). It is located in the TM3 (transmembrane domain 3) that has been associated with channel insensitivity and resistance to abamectin (macrocyclic lactone). Furthermore, the amino acid in the 310 position is very conserved among arthropods (Figure 1.1). It has been reported that a A309V substitution in *Plutella xylostella* GluCl*α* was associated with an 11.000-fold abamectin resistance (Wang *et al.*, 2016) and our substitution is just one amino acid downstream of this mutation (Figure 1.2). This mutation was never found before in field populations *T. urticae* (Papapostolou and Vontas, unpublished data). Thus, the main question is if this mutation generates an abamectin resistance phenotype. This question can be readily addressed by a reverse genetics approach, i.e. generating the mutation in a susceptible genetic background and assessing the resulting phenotype for abamectin resistance. Since such an approach is not yet feasible in spider mites, a model system like *Drosophila* can be used instead.

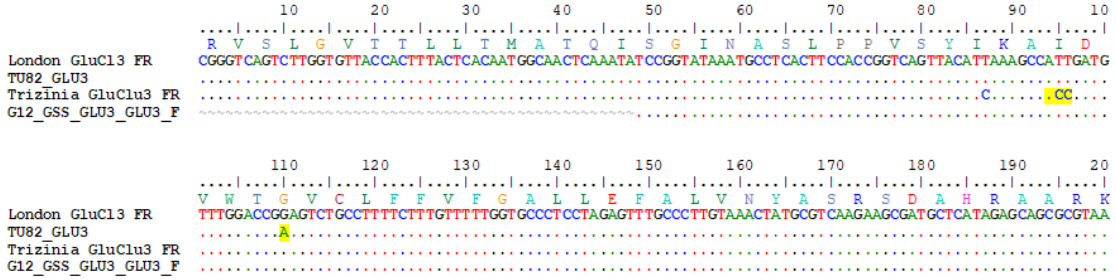

Figure 1.1: Sequencing of GluCl3 in Trizinia population can be seen with an arrow. The position of the substitution is boxed (Papapostolou and Vontas, unpublished data).

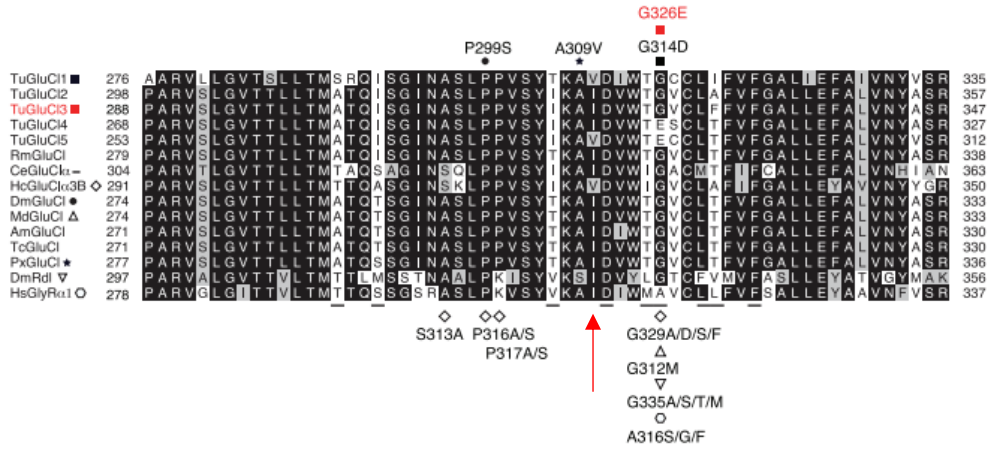

Figure 1.2: Alignment of transmembrane domain 2 and 3 (TM2 and TM3). The position of the novel mutation can be seen with the arrow (Mermans *et al*., 2017).

1.3.3 Genome engineered *Drosophila melanogaster* strains bearing *GluCl3* I310T mutation

CRISPR/ Cas9 is a contemporary and really efficient tool used for genome engineering (Jinek *et al*. 2012). The RNA- guided Cas9 nuclease derived from the microbial clustered regularly interspaced short palindromic repeats (CRISPR) adaptive immune system can be used to facilitate efficient genome engineering in eukaryotic cells by simply specifying a 20- nt targeting sequence within its guide RNA. The repair of double strand breaks (DSBs), which Cas9 generates, are repaired by endogenous cell mechanisms either via homologous- directed repair or via non- homologous end joining. This tool can be used, also, in *Drosophila* for introducing single nucleotide mutations (Bassett, Tibbit *et al.* 2013).

Drosophila is a great tool for functional validation of single nucleotide insecticide resistant mutations identified in different insect species (Douris, Steinbach *et al*. 2016, Douris, Papapostolou *et al*. 2017, Samantsidis, O'Reilly *et al*. 2019). Because the most part of *Drosophila* development and physiology are already known and easily manipulated for genetic screenings, it is a valuable organism for studying the mode of action of various chemical compounds, including insecticides (see reviews by Perry and Batterham, 2018; Homem and Davies, 2018).

1.4 Metabolic resistance: the role of P450s- Functional expression

1.4.1 Insect cytochrome P450s

The large family of cytoxhrome P450s, which are encoded by *CYP* genes, are dispersed in all living organisms from bacteria to humans (Feyereisen, 2012). The number of these genes varies among organisms. In insects *Pediculus humanus* has the fewest (36 *CYP* genes), whereas mosquitoes reach 170 (Feyereisen, 2012). Each *CYP* gene encodes for one P450 enzyme. Their diversity arises from serial gene or genome duplications accompanied by sequence divergence. They are heme- thiolate enzymes with size ranges from 45- to 55- kDa. They are characterized by an absorbance peak near 450 nm of their Fe^{II}- CO complex, and it is because of this feature that they are called P450s. They have various roles (oxidases, reductases, desaturases, isomerases, etc.) but their most prominent is their monooxygenase role. As monooxygenases, they catalyze the transfer of one atom of molecular oxygen to a substrate and reduce the other to water. P450s activity requires, in many cases, redox partners for providing them with reduced equivalents (Feyereisen, 2012).

Insect P450s have been associated with insecticide resistance. Regardless of the number of CYP genes an insect has, they can develop resistance. They are known for xenobiotic metabolism in insects, so they called "detoxification enzymes". A well-known example of insecticide metabolism by P450s is the metabolism of phosphorothioate insecticide (Feyereisen, 2012). Moreover, one well- studied mutation affecting insecticide activity is the transposon insertion in the promoter region of *Cyp6g1*gene in *Drosophila* resulting in overexpression and eventually resistance to DTT and pyrethroids (Daborn, Yen *et al*. 2002).

1.4.2 Functional expression of insect P450s

In order to gain insight of the role of *CYP* genes in resistance, the functional expression of these proteins in heterologous systems is considered necessary. There are several heterologous systems used for P450 functional expression such as *Escherichia coli*, baculovirus, yeast, plant cell suspension cultures, transfection in cell lines and transgenic insects (Feyereisen, 2012). In this study we focused on the baculovirus expression system.

Usually P450s are expressed in baculovirus-infected lepidopteran cells like Sf9. This system has been used for producing large quantities not only for insect P450s but also for mammalian P450s. However, insect P450s expression in a system like this is more advantageous because of the compatible insect endoplasmic reticulum / secretion pathway (Feyereisen, 2012). Heterologous P450s rely for their activity on the function of endogenous P450 reductases. Cases where a second virus expressing a P450 reductase (CPR) is used for co- infection with a virus expressing P450s have been reported (Feyereisen, 2012).

1.5 Scope of this study – questions addressed

The scope of this study is to investigate novel targets for insecticides and investigate insecticide resistance via functional validation and expression. Thus, we wanted to investigate the properties of established lepidopteran midgut cell lines such as transfectability and spheroids formation. Then, we wanted to further characterize the molecular fingerprint of a midgut cell line from *Helicoverpa zea* (RP- HzGUT- AW1) for a series of candidate expression markers and also investigate whether or not the

spheroids form intracellular junctions (sSJs). Furthermore, we tried to establish a protocol for generating a primary midgut cell line from *Helicoverpa armigera* aiming address also there the relevant questions. In parallel, regarding insecticide resistance, we created via CRISPR/ Cas9 a *Drosophila melanogaster* strain for functional validation of I310T alteration found in *Tetranychus urticae* glutamate gated chloride channel. Finally, functional expression of *Apis mellifera* P450s was performed in Sf9 cells using the baculovirus expression system.

2. Materials & Methods

2.1 Establishment of *Helicoverpa armigera* midgut cell line

A number of different protocols were applied for the the establishment of primary cell cultures from the midgut of *H. armigera*. Initially, the protocol used was from Li *et al.* (2015). Then, some modifications have been intoduced based on protocols from Cermenati *et al.* (2007) and Loeb *et al.* (2003). All the solutions and reagents which have been used were according to Li *et al.* (2015).

1st protocol (according to Li *et al.*, 2015):

a) Starvation of five- ten L4 larvae (12 h)
b) Wash of larvae in 70% ethanol containing 1% $NaClO_3$ for 2 min and several washes with ddH_2O.
c) Dissection of larvae under Zoom stereo microscope and wash with lepidopteran physiological solution (LPS) containing 0.001% $NaClO_3$ (six times)
d) Cut midgut with scissors in small pieces, pellet it by centrifugation (1 min at 200× g at room temperature) and wash it with serum free medium to remove cell debris.
e) Resuspension of midgut pieces in Grace's insect medium (Gibco™, ThermoFisher Scientific) supplemented with 15% fetal bovine serum (Gibco™, ThermoFisher Scientific), 50 U/ ml penicillin and 50 μg/ ml streptomycin (Sigma- Aldrich) and culture in wells of six-well tissue culture plates at 26°C.
f) Half of culture medium replacement with 1 ml of fresh medium supplemented with 15% fetal bovine serum, 100 U/ ml penicillin and 100 μg/ ml streptomycin once a week for six- eight weeks.

2nd protocol (modifications according to Cermenati *et al.*, 2007):

Steps (a)- (c) were the same with Li *et al.*, (2015)

d) Pool of 4 midguts into a 70 μm strainer (Falcon® Cell Strainers) in a Petri dish with LPS and mildly agitate for 1 h.
e) Discard sieve, collect free cells in medium, pellet by centrifugation (400× g for 5 min)
f) Resuspend in growth medium (Grace's + 15% FBS + 50 U pen/strep) in 12-well plate at 26°C

3rd protocol (modifications according to Loeb *et al.*, 2003):

Steps (a)- (c) were the same with Li *et al.*, (2015)

d) Incubate 3 opened midguts in standard culture medium (Grace's) for 1 h.

e) Homogenization by pipetting, strain through 70 μm strainers (Falcon® Cell Strainers)
f) Collection of cells by centrifugation (400× g for 5 min)
g) Resuspension of cell pellets in growth medium in 12- well plate at 26°C

Regarding 2nd and 3rd protocol, after two weeks of cultivation, cells were collected, centrifuged, half of the medium was replaced and transferred into wells of six- well plate. Furthermore, every week half of the medium was replaced with 500 μl fresh medium (Grace's + 15% FBS + 50 U pen/strep) and 500 μl conditioned medium (EX-CELL 420 + 10% FBS+ pen/strep) from *Helicoverpa zea* established larval gut cell line (RP- HzGUT- AW1).

2.2 Established insect cell lines

A series of established cell lines, some of which of gut origin, were available to the lab as shown in Table 2.1, and were used in the current study.

Table 2.1 Cultivation conditions of lab available established insect cell lines

Available cell lines	Culture medium	Culture characteristics
Hi5 High Five™ Cells (BTI-TN-5B1-4) (*Trichoplusia ni* embryo)	IPL41 + 10% FBS or Sf-900™ II (Gibco™, ThermoFisher SCIENTIFIC) without FBS	•Mostly floating •Subcultured weekly
Sf9 (*Spodoptera frugiperda*) (embryo)	Sf- 900™ II (Gibco™, ThermoFisher SCIENTIFIC) + 10% FBS (Gibco™, ThermoFisher SCIENTIFIC)	•Subcultured weekly •Serum: Multiple layers forming. Monolayer detached with cell scraper. Subcultured only when more than 100% confluent •Serum-free: Attach only after subculture
Cf1 (*Choristoneura fumiferana*)	Sf- 900™ II (Gibco™, ThermoFisher SCIENTIFIC) + 10% FBS	•Fast growth •Forming of large "mats" when highly concentrated •Easily disrupted monolayer
Cf203- 900 (*Choristoneura fumiferana*) (midgut)	SF900™ 1.3× (Gibco™, ThermoFisher SCIENTIFIC) + 10% FBS + L-Glutamine	•Monolayer forming •Monolayer detached with cell scraper or trypsin •Subcultured every 3-4 days
RP-HzGUT-AW1 or AW1 (*Helicoverpa zea*) (larval gut)	EX-CELL® 420 (Sigma-Aldrich) + 10% heat inactivated FBS + penicillin/streptomycin 100× (Sigma- Aldrich)	•Fast growth •Subcultured weekly •Floating and attaching cells
BCIRL-HzMG8 or MG8 (*Helicoverpa zea*) (midgut)	EX-CELL® 420 (Sigma-Aldrich) (serum-free)	•Floating cells •Subcultured weekly

BCIRL-AtE-CLG15A or CLG15A (*Anasa tristis:* Hemiptera) (eggs)	EX-CELL® 420 (Sigma-Aldrich) + L15 Liebovitz' medium (Sigma- Aldrich) (1:1), + 10% FBS + 100× penicillin/streptomycin	•Fibroblast-like attaching cells •Subculture weekly •Monolayer detached with cell scraper or trypsin

2.3 Generation of pEIA- EGFP plasmid

The original pEIA vector (Douris *et al.*, 2006) contains an Actin promoter from the silkworm *Bombyx mori* and two baculoviral elements, the *hr3* enhancer sequence and the IE1 transactivator cassette. In order to generate marker plasmid pEIA.EGFP to be used for transfection of established cell lines, the following steps were followed:

a) Transformation of pBac [3xP3- EGFPaf] plasmid, from which EGFP sequence should be taken and inserted in another plasmid (pEIA), in DH5α *Escherichia coli* cells.
b) Isolation of high- copy plasmid DNA from *E. coli* (NucleoSpin® Plasmid/ Plasmid (NoLid) protocols- MACHEREY- NAGEL)
c) Double digestion with BamHI and NotI of pBac [3xP3- EGFPaf] plasmid (insert) and pEIA plasmid (vector). The EGFP ORF should be inserted downstream of the actin promoter in pEIA plasmid (Fig. 2.1). Between actin promoter and SV 40 terminator there is a multiple cloning site, where BamHI and NotI cut. NotI cuts at 3' end of EGFP gene, whereas BamHI cuts at 5' end. No one of these enzymes cuts inside the gene, so they are suitable for the digestion.
d) Run digestion products at an 1.5% w/v agarose gel, select and cut the correct bands from the gel
e) Gel extraction (MACHEREY- NAGEL) for isolation of insert and vector.
f) Ligation of insert and vector (New England BioLabs)
g) Transformation of the newly generated plasmid in DH5α *Escherichia coli* cells.
h) Screening colony PCR with EGFP specific primers
i) Grow the correct new generated plasmid and perform midipreps (NucleoBond® Xtra Midi/ Maxi- MACHEREY- NAGEL)
j) Check if the plasmid is the desirable one with diagnostic PCR and/ or sequencing.

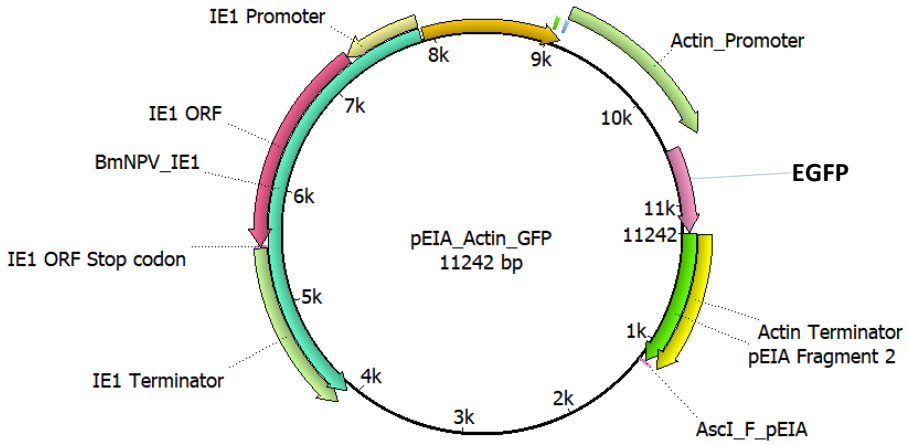

Figure 2.1: pEIA_ EGFP plaσmid. All the regulatory elements are depicted in the figure. The plasmid is 11242 bp long.

2.4 Transfection of established cell lines

Transfections were performed in several cell lines (Hi5 serum free (Hi5-SF), Cf1, Cf203- 900, AW1 and CLG15A, see Table 2.1), following a standard protocol of transfection for ESCORT^{TM} IV transfection reagent (lipofectin) (Sigma- Aldrich) as follows:

.

a) Seed cells in 800 µl serum free medium 1- 2 days before transfection to achieve 50- 70% confluence at the time of transfection in wells of a 6- well plate.
b) Preparation of transfection mix; use 1.5 ml Eppendorf tubes (2 tubes for each cell line).
   Solution A: for each transfection, dilute 1 or 2 µg of plasmid into 100 µl serum free medium.
   Solution B: for each transfection, dilute 5 or 10 µl of lipofectin into 100 µl serum free medium.
c) Add solution A to the corresponding tubes of solution B and gently mix by pipetting the liquid up and down. Allow the DNA/ liposome complexes to form for 45 min at room temperature.
d) Add the DNA / liposome complex solutions (200 µl) to the corresponding wells of 6- well plate in a dropwise manner, trying to cover all the areas of the well. Mix by gently swirling the plates. Incubate the cells for 6 hours at 27^{o} C.
e) Add 1ml of complete medium, containing twice as much serum and antibiotics as normally used to grow the cells. This attenuates the transfection and restores the serum and antibiotic concentrations to normal levels.
f) Incubate cells for additional 24 h at 27^{o} C. Aspirate the medium and replace it with complete medium.
g) Incubate cells in a 27^{o} C incubator for 2-4 days.
h) Take photos of transfected cells at 48, 72 and 96 h post transfection.

2.5 Generation of hanging drops (spheroids)

a) Pass cells from syringe with 21G needle before seeding for hanging drops
b) Count cells so each drop of 20 μl should contain 500 cells
c) Use multi- channel pipette to pipette 20 μl drops on the lid of a Petri plate.
d) Add 10 ml of 1× PBS in the Petri plate to avoid evaporation of drops
e) Invert the plate quickly without disturbing the drops
f) Put the plate in a 26° C incubator carefully without disturbing the drops
g) Observe under an inverted microscope and collect the drops after a week.

2.6 Preparation of samples for transcriptomics

2.6.1 RNA extraction with TRI Reagent® (Molecular Research Center, Inc- MRC)

a) Homogenize cells by pipetting up/ down in 500 μl TRI Reagent®
b) Centrifuge for 15 min at 15000× g at 4° C.
c) Transfer supernatant in a new 1,5 ml Eppendorf tube and add 1/5 of TRI Reagent® volume, chloroform (100 μl)
d) Invert it (up/ down) for 15- 20 sec and let it stand for 5 min at room temperature
e) Centrifuge for 15 min at 15000× g at 4° C.
f) Collect the upper phase carefully, transfer it into a new 1,5 ml Eppendorf tube and add 1/5 of the initial volume ice- cold isopropanol (100 μl)
g) Invert (up/ down) the tube and let it stand for 10 min at room temperature
h) Centrifuge for 15 min at 20000× g at 4° C.
i) Remove supernatant and wash the pellet with 500 μl 70% ethanol
j) Centrifuge for 15 min at 20000× g at 4° C. If the pellet is colored repeat the previous step once more.
k) Remove carefully ethanol and let air- dry pellet for 5- 10 min
l) Dissolve pellet in 20 μl dH_2O and let it stand on ice
m) After 30 min on ice, pellet was completely dissolved and the concentration was measured at Nanodrop.
n) DNase treatment with TURBO™ DNase (2 U/μl) (Invitrogen)
    i. Add 10× Turbo DNase buffer and 1 μl TURBO™ DNase to the RNA and mix gently by pipetting up/ down
    ii. Incubate at 37° C in the waterbath for 30 min.
    iii. Add 0.1 volume of DNase inactivation reagent and mix well by pipetting up/ down.
    iv. Incubate at room temperature for 5 min and mix occasionally.
    v. Centrifuge at 10000× g for 1,5 min at room temperature
    vi. Transfer carefully upper clean phase to a new 1.5 ml Eppendorf tube
    vii. Measure new concentration at Nanodrop
    viii. Run 500- 1000 ng of RNA in 1.5% agarose gel to check the quality of RNA.

2.6.2 cDNA synthesis using MINOTECH reverse transcriptase (RT)

a) Create two master mixes. In the first master mix add: 1 μl oligo(dT) 20 (50 μM), 10 pg- 5 μg total RNA, 1 μl 10 mM dNTP mix, sterile ultrapure water up to 13 μl.

b) Heat mixture to 65° C for 5 min
c) Incubate on ice for at least 1 min
d) Brief centrifugation and add the second master mix which contains 4 μl 5× MINOTECH RT assay buffer, 1 μl 0.1 M DTT, 1 μl RNase Inhibitor (40 U/ μl) and 1 μl of MINOTECH RT (200 U/ μl).
e) Mix gently.
f) Incubate at 42° C for 60 min.
g) Heat inactivation step at 70° C for 15 min.
h) After cDNA synthesis, next step is PCR with MINOTECH Taq DNA polymerase (5 U/μl). The reagents which are required for a 20 μl reaction are: 2 μl MINOTECH Taq pol. Buffer, 0.4 μl 10 mM dNTP mix, 0.4 μl 10 μM forward primer, 0.4 μl 10 μM reverse primer, 1 μl cDNA, 0.1 MINOTECH Taq DNA pol. and 15.7 μl dH_2O

2.7 *Drosophila* strains used for CRISPR and subsequent crosses

The injections for genome modification of *Drosophila* were performed in eggs of the lab strain y1 M{nos-Cas9.P} ZH-2A w*, in which the endonuclease Cas9 is expressed under the control of the promoting element *nos* (further below referred as nos-Cas9; #54591 in the Bloomington *Drosophila* stock center, Port *et al*., 2014). Moreover, this strain was used for outcrossing individually the G_0 adults generated from the injections. Strain yw; TM3 *Sb e*/TM6B *Tb Hu e* (balancer stock was kindly provided by professor Christos Delidakis, IMBB and University of Crete) which contains two third chromosome balancers (TM3 & TM6B, further below referred as TM3/ TM6B) and the phenotypic markers Stubble (short bristles) and Tubby (barrel- shaped body) respectively, was used for genetic crosses and for keeping the mutations at heterozygous state. The flies were cultured at 25°C temperature, at 60-70% humidity and 12:12 hour photoperiod on a standard fly diet.

2.8 Strategy of genome editing

The CRISPR/ Cas9 strategy was designed in order to generate a single mutation (relevant to the ones found in *T. urticae*, I310T) in the *GluCl* gene of nanos-Cas9. For this reason, a construct was designed bearing the I310T mutation (further below referred as IT). The constructs which were used for CRISPR mediated substitutions in *GluCl* gene are depicted in figure 2.2. Initially, the sequence of *GluCl* gene of nanos-Cas9 strain was obtained in order to design the desired mutation. The sequencing of *glutamate chloride channel (GluCl)* gene in the nanos-Cas9 strain genome has been performed in previous projects of Vontas lab (Iason Christou, MSc thesis). Based on this sequence, several CRISPR targets in the desired region were identified by using the online tool Optimal Target Finder (Gratz *et al.,* 2014) (http://tools.flycrispr.molbio.wisc.edu/targetFinder). The target which was selected, contained the nucleotides of the desired modification with no predicted off-target

effects. Relevant to this target, an RNA expressing plasmid was constructed. In particular, two single stranded, 5' phosphorylated oligos (sense oligo: 5'-CTTCGAAGGCCATCGATGTGTGGAC-3' & antisense oligo: 5'-AAACGTCCACACATCGATGGCCTTC-3') were designed according to the target region and ordered from Invitrogen. These ssDNA oligos were used in order to generate a double stranded DNA oligo (dsDNA oligo) by annealing, in order to acquire a dsDNA oligo for the guide RNA that had 5' and 3' single stranded overhangs based on the sequence of the sticky ends that digestion with BbsI enzyme generates. These overhangs were generated in order to facilitate ligation into dephosphorylated gRNA vector pU6-BbsI chiRNA (Gratz *et al*., 2013), after digestion with BbsI. Following ligation, the constructs were transformed into DH5α competent cells following the standard protocol of transformation. After overnight culturing, 5 single colonies from each construct were picked and they were checked for the insert by performing colony PCR using T7 universal primer and the antisense oligo for each dsDNA. The sequence of each construct was checked by sequencing (Macrogen sequencing facility, Amsterdam). To facilitate Homologous Directed Repair (HDR) we had to construct a *de novo* (Genescript) donor plasmid (see Sup. Fig. 1) which contained two ~800bp homology arms flanking the CRISPR target. The target region (Fig. 2.2) was designed to contain several synonymous mutations (extra from the main desired non-synonymous mutation), which served two purposes: a) generate diagnostic markers in order to facilitate the screening of the CRISPR events and b) mutations in the gRNA and in the PAM sequence in order to prevent CRISPR induced DSB in the donor plasmid and/or HDR-modified flies. Thus, the target region (Fig. 2.2) in the donor template was designed in order to abolish a ClaI restriction site and introduce a new MluI restriction site that help differentiate between genome modified and wild-type alleles in simple diagnostic assays.

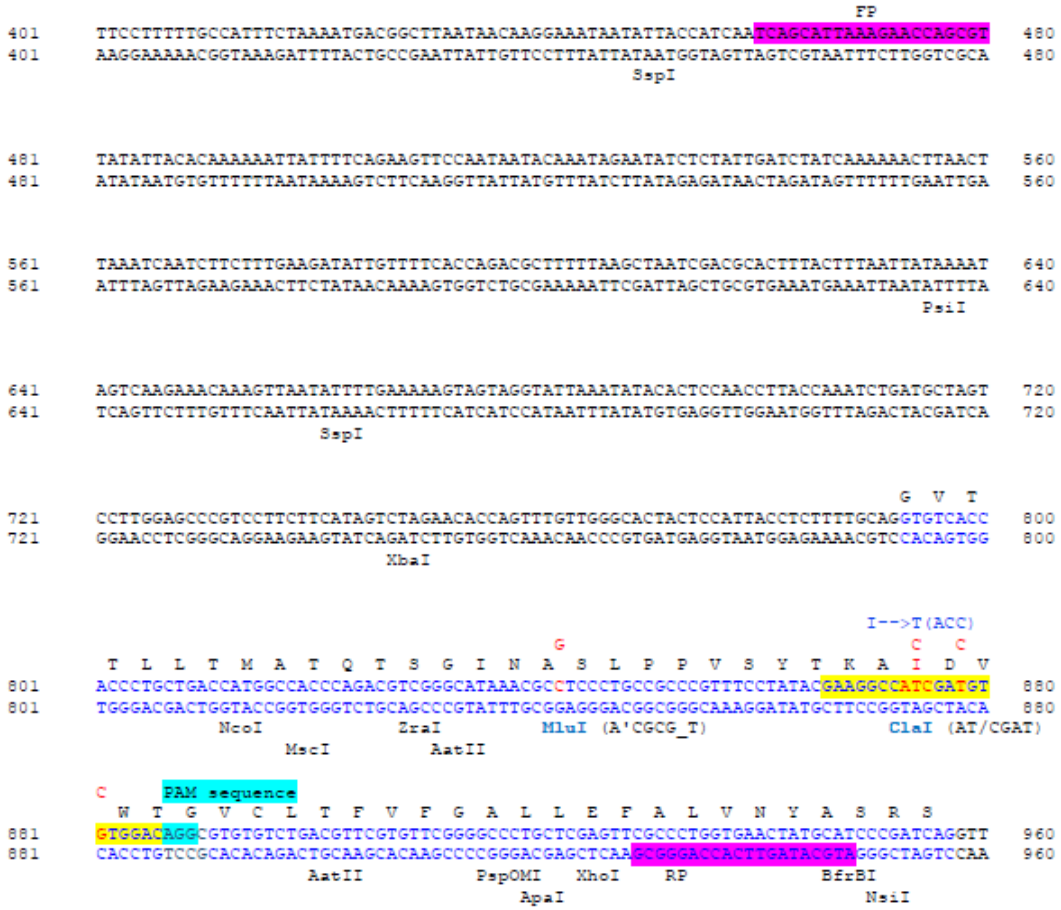

Figure 2.2: Nucleotide sequence of the *glutamate chloride* gene region used in order to generate CRISPR mediated mutant flies bearing I310T. Highlighting with yellow indicates the gRNA GluCl target sequence. The blue highlighting indicates the PAM sequence in 5'→3' direction. Highlighted sequences with pink refer to the forward (FP) and reverse (RP) generic primers used for the PCR reactions as diagnostics. The FP has been, also, used in pair with the reverse specific primer. The reverse specific primer sequence which is on the mutation is shown in yellow. The synonymous substitutions which have been made in donor plasmid for creating a restriction site for MluI and for protecting the gRNA target sequence from CRISPR/Cas9 cleavage are shown in red color with their substitutes above them. The enzymes which have been used for diagnostics are under the sequence and with blue letters (MluI & ClaI). Black letters show the intron area whereas blue letters the exon area.

2.9 DNA extraction with DNAzol (Molecular Research Center, Inc.- MRC) from pools of pupae or individual adult flies

a) Grind fly in 200 µl DNAzol (500 µl for pupae)
b) Centrifuge at 10000 rpm for 10 min at room temperature (20 min at pupae)
c) Transfer supernatant into a new 1.5 ml Eppendorf tube
d) Add 100 µl (250 µl for pupae) 100% v/v ethanol. Mix well by repeatedly inverting the tube
e) Centrifuge at 13000 rpm for 20 min at room temperature
f) Discard supernatant
g) Wash DNA pellet with 800 µl 75% v/v ethanol
h) Centrifuge at 13000 rpm for 5 min at room temperature

i) Discard supernatant and spin down
j) Air dry pellet for 30 min at room temperature
k) Resuspend in 20 μl (100 μl for pupae) dH_2O and vortex

2.10 Screening and genetic crosses for the generation of genome modified flies

Injection of approximately 500 *Drosophila* eggs (nanos-Cas9 strain) was performed by Ioannis Livadaras (IMBB/FORTH) with an injection mix containing at final concentration 75ng/ μl of the gRNA expressing vector and 100ng/ μl of donor template, 10× injection buffer and dH_2O. First instar larvae were collected 24 and 48 hours after injection. The larvae were transferred into standard fly artificial diet. After 9-13 days, fly adults were collected and they were backcrossed individually with nos-Cas9 strain (each individual cross was taken as a different line). Pupae of G_1 of each line were pooled into batches of 30 and genomic DNA (gDNA) extraction was performed in order for them to be screened with two different methods. The first method is to digest 2μg of gDNA with ClaI (New England BioLabs), which cuts the wild type sequence for reducing (or eliminating of possible) the amplification of the wild type allele, followed by PCR with generic primers and then digest again with MluI (New England Biolabs) that cuts only the mutated sequence to verify that the product is derived from the genome modified allele. The second method is after cutting with ClaI (or even without cutting at all) to amplify with specific primers the region with the desired mutation. Generic primers (Sup. Table 1) give an amplicon of 489 bp whereas specific primers (Sup. Table 1) give an amplicon of 429 bp. Digestions were performed as shown in Table 2.2.

Table 2.2: Protocol of digestion.

Digestions' protocols (2 h at 37º C)	
Reagents ×1 ClaI (New England Biolabs)	Reagents ×1 MluI (New England Biolabs)
2 μl CutSmart® Buffer	2 μl NEBuffer™ 3.1
2 μg DNA template	5 μl PCR template
0,5 μl enzyme ClaI	1.5 μl enzyme MluI
dH_2O up to 20 μl	11.5 μl dH_2O
20 μl total volume	20 μl total volume

The crossing scheme for the generation of homozygous lines is shown in Figure 2.3. G_1 flies from the same original cross positive for the mutations were backcrossed individually with nos.Cas9, in order to generate the G_2 generation. Each G_1 fly was screened individually and crosses positive for the modification were established. Approximately 50% of the G_2 generation from these crosses is expected to be positive for the mutations. Individual G_2 flies were crossed with flies carrying balancer chromosomes for the third chromosome (TM3/ TM6B). G_2 flies crossed over TM3/ TM6B were individually screened for establishing the positive G_3 progeny lines against the balancer chromosome. Then, single flies derived by the G_3 progeny (50% of the progeny contain the modified allele against balancer) with Stubble marker (TM3) were

selected and back-crossed with the same balancer fly stock. Final molecular screening was carried out, and adults with Stubble phenotype from the positive lines (heterozygous for the mutation) were collected and crossed among themselves in order to take several homozygous flies for the establishment of a genome modified homozygous population. DNA was extracted from homozygous male and female adults and amplified by using generic primers (see Sup. Table 1) yielding a fragment of 489 bp, which was then purified and sent for sequencing (Macrogen Sequencing Facility, Amsterdam). Each experiment concerning the molecular screening of the modified flies was performed along with positive control (the donor plasmids used for the injections), negative control (the gDNA of nos-Cas9) and blank (no template). PCR conditions are shown in Table 2.3.

Table 2.3: PCR conditions

PCR with generic/ specific primers		
Reagents	×1 (μl)	PCR conditions
10× Minotech Taq pol. buffer	2	Initial denaturation → 94° C, 2 min **[**Denature→ 94° C, 45 sec Anneal→ 57° C (generic primers) or 51°C (specific primers), 30 sec Extend→ 72° C, 30 sec**]**×35 cycles Final extension→ 72° C, 5 min Hold→ 4° C, indefinitely
10 mM dNTP mix	0.4	
10 μM forward primer	0.4	
10 μM reverse primer	0.4	
DNA template	1	
MINOTECH Taq DNA pol. (5u/ μl)	0.1	
dH_2O	15.7	
Total volume	20	

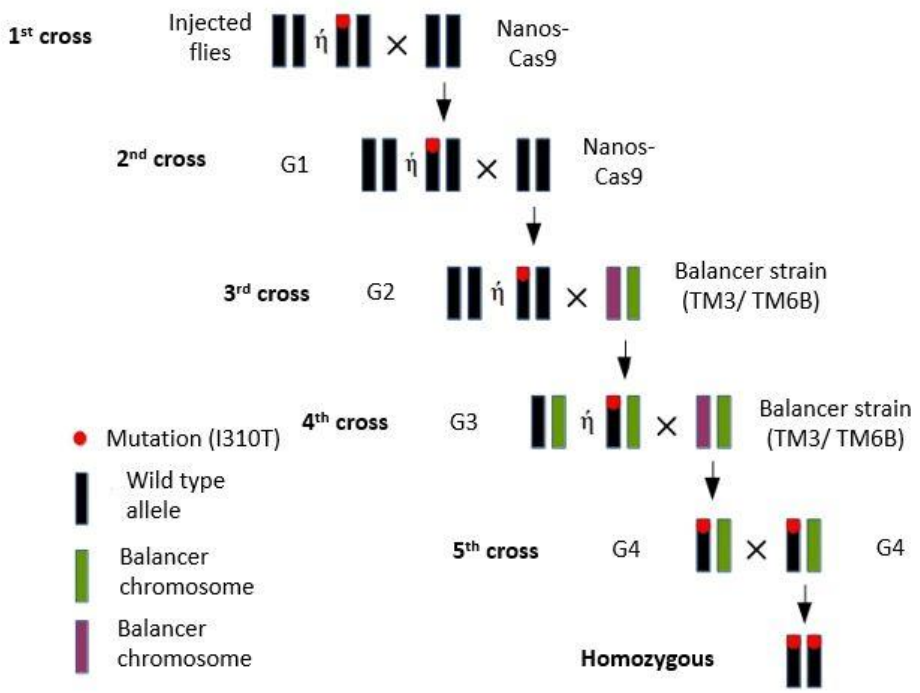

Figure 2.3: Figure adapted from R. Panteleri M.Sc thesis, Department of Chemistry, University of Crete. The fly crosses flowchart. Wild type alleles (black), balancer strain with two balancers (TM3/ TM6B) chromosomes (green & purple) and the mutation (I310T) of *GluCl* gene (red dot). The progeny of 1st cross is screened in pools. In next crosses, parents are screened after they have given progeny. For the next crosses the progeny from positive for the mutation parents is used. After the 3rd cross, one of two phenotypic markers (which arise from crosses with balancer) is selected, usually the most distinct. *GluCl* gene is located in the 3rd pair of *D. melanogaster* chromosomes.

2.11 Sf9 insect cells

Sf9 cell line (Invitrogen) has been established from ovarian tissue. It is a clonal isolate of *Spodoptera frugiperda* Sf21 cells (IPLB- Sf21- AE) and is commonly used in insect cell culture for recombinant protein production using baculovirus. As for cell line growth, it can be cultured with or without serum and attached or in suspension.

2.12 Transfection of Sf9 cells with recombinant bacmid DNA

Three P450s were used (CYP9Q1-3) (Manjon, *et al*. 2018). For BACmids generation pFASTBac CT TOPO kit was used. The BACmids were prepared by Dr Maria Riga.

i) Seed 10^6 cells per well in 6- well plate in 800 μl serum and antibiotics free Sf- 900™ II (Gibco™, ThermoFisher SCIENTIFIC) culture medium after washing them twice with the same medium and let them attach at 27° C for at least 1 h.

ii) Preparation of transfection mix; use 12× 1.5 ml Eppendorf tubes (2 tubes for each expression of recombinant protein of interest; CYP9Q1-3, AgCPR, GFP and mock)

Solution A (6 tubes): for each transfection, dilute 2 μg of Bacmid DNA into 100 μl SF- 900 II SFM without serum and antibiotics.

Solution B (6 tubes): for each transfection, dilute 10 μl of ESCORT^{TM} IV Transfection Reagent (Sigma- Aldrich) into 100 μl SF- 900 II SFM without serum and antibiotics.
iii) Add solution A to the corresponding tubes of solution B and gently mix by pipetting the liquid up and down. Allow the DNA/ liposome complexes to form for 45 min at room temperature.
iv) Add the DNA / liposome complex solutions (200 μl) to the corresponding wells of 6- well plate in a dropwise manner, trying to cover all the areas of the well. Mix by gently swirling the plates. Incubate the cells for 6 hours at 27^{o} C.
v) Add 1ml of complete medium; SF900 II SFM + 10% fetal bovine serum (FBS), Gibco, ThermoFisher Scientific, containing twice as much serum and antibiotics as normally used to grow the cells. This attenuates the transfection and restores the serum and antibiotic concentrations to normal levels.
vi) Incubate cells for additional 24 h at 27^{o} C. Aspirate the medium and replace it with complete medium. Put the plate in closed box with wet kimwipe on the bottom to prevent media evaporation. Incubate cells in a 27^{o} C incubator for 4-5 days.
vii) After 5 days collect the cells and the medium, centrifuge them at 12000 rpm for 5 min at room temperature. Transfer the supernatant, which contains the virus (P0), in a new tube and store it at 4^{o} C protected from light. Keep the pellet (cells) for performing SDS-PAGE to verify expression of recombinant protein.
viii) Use 10 μl of each supernatant for further amplification of each virus in 5 ml Sf9 cells in T25 flasks and incubate them at 27^{o} C for a week.
ix) Collect supernatant- amplified virus (P1) (centrifugation at 12000 rpm for 5 min) at a 15 ml tube and store it at 4^{o} C protected from light.

2.13 Virus titration
i) Preparation of 8 serial dilutions of each virus; The first dilution (A) is the P1. 100 μl of P1 are diluted in 900 μl complete medium (SF900 II SFM + 10% FBS) and vortexed, this is the second dilution (B). The rest of the dilutions (C-H) are generated in the same way by adding 100 μl of previous dilution to 900 μl complete medium.
ii) Seed in 96- well plates 10^4 SF9 cells in complete medium in each well in a final volume of 200 μl.
iii) Add in the first ten wells of each row of 96- well plate 10 μl of the same dilution of the virus, creating 10 replicates for each dilution. Each row of the 96- well plate is matched to a different dilution. The two last wells of each row contain only cells and are used as negative controls.
iv) Put the 96-well plates in closed box with wet kimwipe on the bottom to prevent media evaporation. Incubate cells in 27^{o} C and after at least 48 h observe them in microscope.
v) Notice in which dilution (row) the cells are dead in all the wells, are all alive and between which two titers the half of the wells contain dead cells and the rest of them alive cells.
vi) Use an online $TCID_{50}$ calculator (© Marco Binder, Dept. Infectious Diseases, Molecular Virology, Heidelberg University) for initial concentration of viruses (FFU/ ml). $TCID_{50}$ is calculated by the Spearman & Kärber algorithm as described in Hierholzer & Killington (1996).

2.14 Co- infection of CYP9Q1-3 with AgCPR

i) Add according to the literature (Gong *et al.*, 2017) the sutitable ratio of virus combination CYP9Q1-3 and AgCPR in the same T25 flask for co- expression. The optimum ratio for the co- expression of the P450/ CPR- recombinant baculovirus in Sf9 was 10:1 (MOI: 0.5 for P450 and 0.05 for CPR) according to Gong *et al.*, 2017.
ii) Add, 24 h after coinfection, 1 μg/ml hemin and 0.1 mM 5- ALA in each flask.
iii) Collect cells 72 h after co- infection and use them for downstream assays.
iv) Perform co- infections in T75 flasks for protein expression scale up.

2.15 Protein extraction

i)Collect 1 ml cells 72h after co- infection, centrifuge at 1000 rpm for 3 min and wash them three times with ice- cold 1× PBS. Then, resuspend each pellet by pipetting in 200 μl RIPA + 100× protease inhibitors in 2 ml tubes. Freeze and thaw; put the tubes in liquid nitrogen until you will hear a characteristic sound and then put them in a waterbath at 37^{o} C until the sample melts. Repeat this procedure for five times. Add 50 μl 5× protein loading buffer and β- mercaptoethanol in each sample, boil at 95^{o} C for 5 min and spin at 14000 rpm for 5 min. Store the samples at – 20^{o} C or dilute them (1/5 in final volume of 100 μl) and load them at gels.
ii) Preparation of 12% acrylamide gels (stacking gel and 12% separating gel):
iii) Load 10 μl of each sample and 5 μl prestained marker at gels and run at 100 Volt constantly.

2.16 Western blot

a) Transfer: Prepare the 'sandwich' with gel and nitrocellulose membrane, put it in the suitable device and then run at 350 mA constantly for 1 h
b) Staining the membrane with Ponceau S stain for 1 min and then rinse with dH_2O to see the migration profile of samples. Wash the membrane with PBS-T to remove the rest of stain.
c) Probing:

i) Blocking the membranes for 1 h at room temperature in 5% milk in PBS-T

ii) Rinse in PBS-T

iii) Apply 1 ml of primary antibodies in each membrane, enclose in plastic bag and let them rotate overnight at 4^{o} C (Table 2.4).

iv) Keep the primary antibody in a tube at - 20^{o} C and then wash 3× with PBS-T for 5 min each.

v) Apply secondary antibody and let it rotate for 1h at room temperature (Table 2.4).

vi) Remove secondary antibody and then wash 3× with PBS-T for 5 min each.

vii) Detection of proteins with chemiluminescent method using ThermoFisher Scientiifc ECL Western Blotting Substrate. Apply 1:1 ECL mix on membrane (750 μl for each membrane) and spread it with a blue tip. Transfer it to the cassette and developing.

Table 2.4: Antibodies used and their dilution conditions

Primary antibodies	Dilution	Secondary antibodies	Dilution
Anti- His mouse Qiagen	1:1000 in 3% milk	Anti- mouse HRP	1/10000 in 3% milk
Anti- CPR rabbit Qiagen	1:1000 rabbit in 1% milk	Anti- rabbit HRP	1/10000 in 3% milk

2.17 Preparation of microsomal proteins

Whole cell lysate protein was collected 72 h after co-infection. The cells were prepared by pelleting them at 1000 × g for 10 min at 4 °C, followed by washing twice with ice-cold PBS buffer (pH 7.4), and re-suspension in homogenization buffer (0.1 M phosphate (pH 7.4), 1.0 mM EDTA, 0.25 M sucrose and 0.5 mM PMSF). They were then homogenized by sonication for 12 seconds, after which the crude homogenate was centrifuged at 8000 × g for 10 min at 4 °C followed by ultracentrifugation (SORVAll) at 80.000 rpm for 60 min at 4 °C. The resulting microsomal protein pellets were re-suspended in resuspension buffer (0.1 M phosphate buffer pH 7.4, 20% glycerol buffer, 1 mM EDTA, 0.1 mM DTT, 1 mM PMSF) containing a protease inhibitor cocktail and stored at −80 °C until use (Gong, Li *et al.* 2017).

2.18 CO spectrum assay

a) Add in cuvettes 1 ml CO buffer (100 mM Tris- HCl pH7.4, 20% glycerol, 1 mM EDTA and dH_2O) and a reducing agent (sodium hydrosulfite)
b) Stir and add a protein amount. Here 15 μl of protein were added because it was high-concentrated. This is the blank before we add CO
c) Measure blank at 400- 500 nm every 2 nm
d) Add CO in the sample for 45 sec and stir
e) Measure again at 400- 500 nm every 2 nm
f) Repeat steps (d) & (e)
g) Increase the protein amount at 30 μl and then repeat all the procedure

2.19 CPR activity determination

CPR activity was determined using the method recommended by Liu & Scott (1996) with slight modifications. A cytochrome c assay was used to determine the activity of CPR. Briefly, microsomal protein was placed in a cuvette to which 500 nM cytochrome c was added and the baseline recorded. The initial rate of the cytochrome c reduction was monitored at 550 nm for 1 min after 0.05 mM NADPH (provides energy to the system) was added and immediately mixed, using a UV/visible spectrophotometer. Activity is expressed here as units per milligram protein, with one unit of reductase activity defined as 1 nmol cytochrome c reduced per minute. The velocity has been estimated from a kinetic curve.

The biochemical assays which are reported in sections 2.17, 2.18 and 2.19 were performed by Dimitra Tsakireli, lab technician.

3.Results

3.1 Insect cell based assays for drug discovery

A major goal of this study is to investigate insect cell based assays for drug discovery using either primary midgut cells of *Helicoverpa armigera* or already established cell lines (midgut or non- midgut origin) derived from other lepidopteran species. The project is organized along two main objectives. The first one is the establishment of primary midgut cell cultures derived from *H. armigera*, examination of the properties of these cultures and its potential for downstream assays similar to the Caco- 2 assay used in mammalian cells. The second objective is about investigation of the properties of the already established cell lines (Table 2.1) such as viability, growth rate, proliferation, transfectability, ability of forming spheroids and monolayer. Last, but not least, both objectives were facilitated by investigating the use of certain midgut specific genes as marker genes for the determination of cell type specificity and developmental profile.

3.1.1 Primary midgut cell culture of *Helicoverpa armigera*

Initial efforts for establishment of a primary midgut cell culture were performed using the 1st protocol (according to Li *et al.*, 2015) described in 2.1. After dissection the cells were maintained in culture for 8 weeks. During these weeks, there was not any significant progress in development (no significant growth rate and proliferation). Although all the different midgut cell types were observed. As seen in Figure 3.1, intestinal stem cells (ISCs), columnar cells or enterocytes (ECs) and Goblet cells (GCs) existed in the culture. There is also a fourth midgut cell type the enteroendocrine cells (EEs) which are not easily detected by morphology alone. After four weeks of culture, the cells started to die gradually and the culture was contaminated with bacteria and fungi.

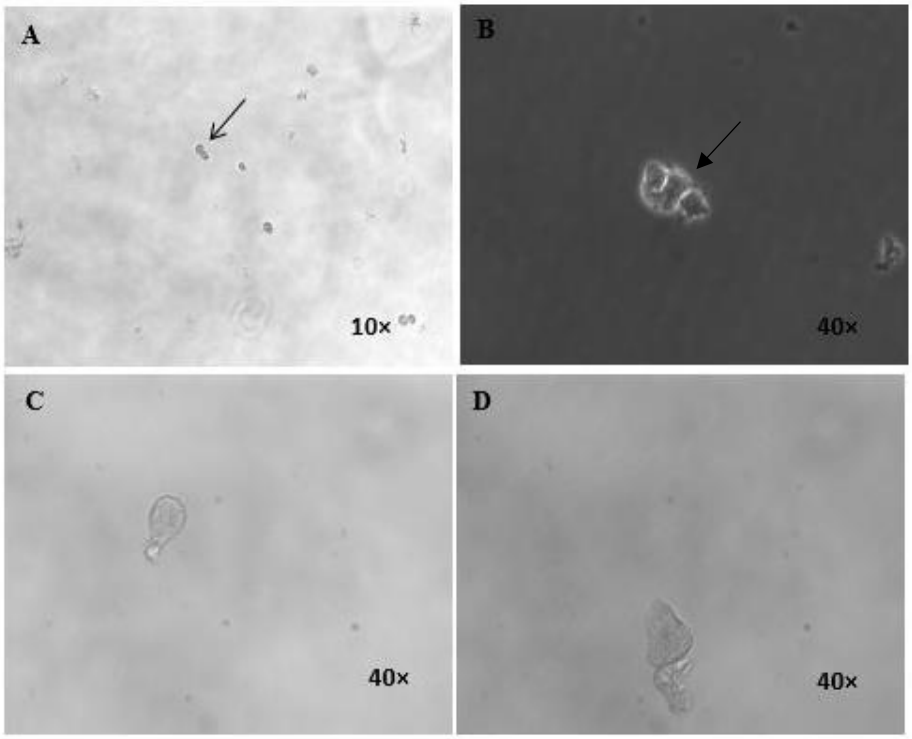

Figure 3. 1: Different cell types of *H. armigera* midgut. (A) ISCs during duplication 10× zoom of lens. (B) & (D) Enterocyte (arrow) under 40× zoom of lens. The brush border of enterocyte is also evident. (C) Pear- shaped Goblet cell under 40× zoom of lens.

As it is shown in Figure 3.1, the ISCs are round shaped (Fig. 3.1A) whereas GCs are pear- shaped and ECs are more square-like. ECs possess the distinctive brush border structure.

In order to facilitate growth and investigate further options, we used the 2nd protocol (according to Cermenati *et al.*, 2007) & 3rd protocol (according to Loeb *et al.*, 2003) with some modifications as described in 2.1. These modifications regard the use of strainers and conditioning of the growth medium with cell supeprnatant from a *H. zea* midgut cell line (AW1). In Figure 3.2 there are photographs of primary cells grown for up to10 weeks after dissection using both protocols. Two weeks after dissection the cells from each protocol were collected from the wells of the 12-well plate and were split each in two wells of a 6- well plate (Fig.3.2 C & C'). Each culture contained definitely the three identifiable midgut cell types (ISCs, ECs & GCs). We were not able to recognize EEs from the other cell types, since they do not have any special morphology. Cells which have been isolated by following protocol 2 were less in number but it was easier to observe the different cell types whereas the cells from protocol 3 were denser and their morphology was less clear. After the 4th week of culture (Fig. 3.2 E-J & E'-J') cells started to proliferate with higher rate, some of them attached to the bottom and formed clumps. Ten weeks after the first cultivation no contamination was observed. In Fig. 3.2 E', the arrow shows a cell with a double nucleus during mitosis.

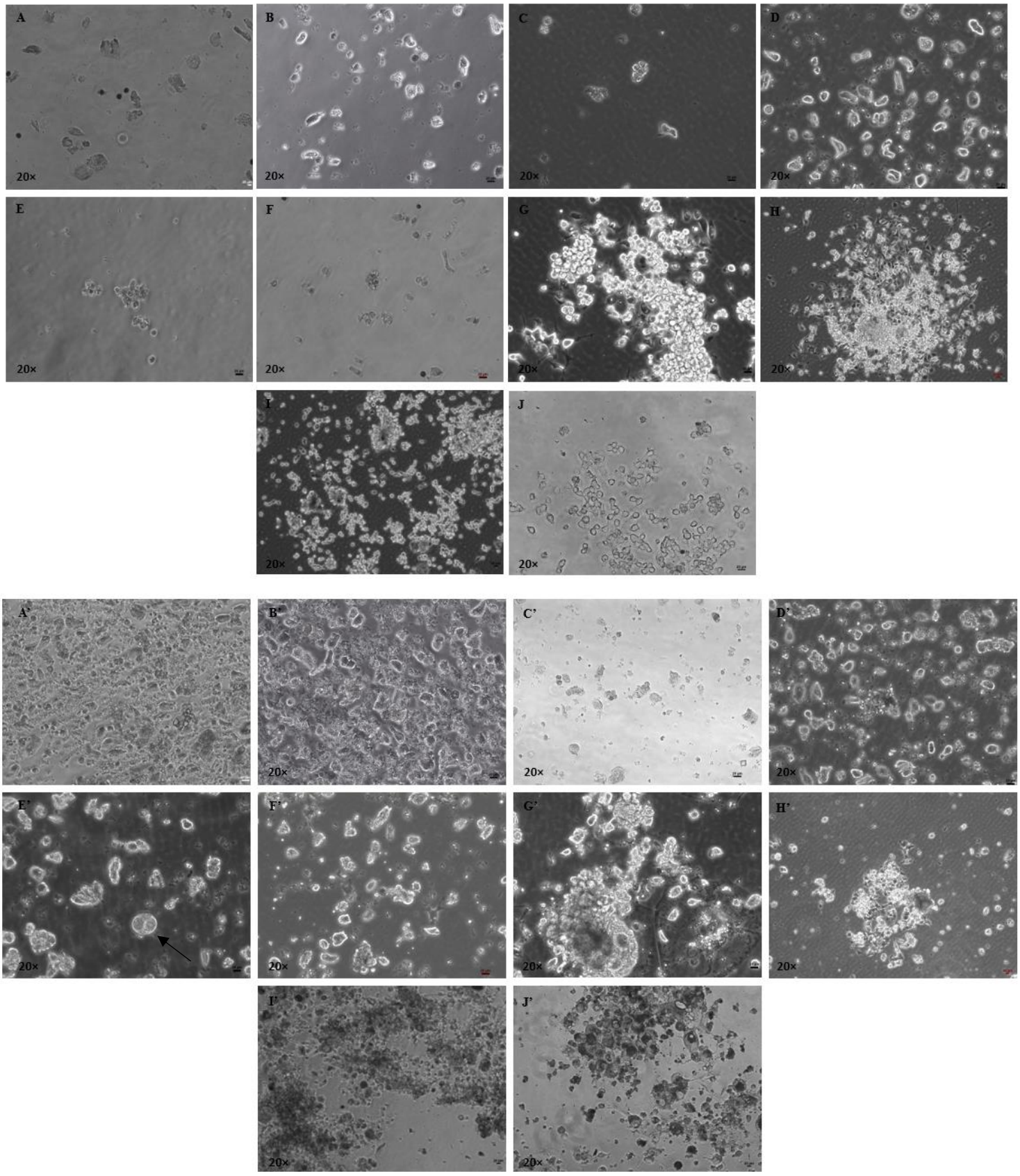

Figure 3.2: Midgut primary cell line progress using two different protocols Cermenati *et al*. (2007) (A-J) & Loeb *et al*. (2003) (A'-J'). (A) & (A') 1st week after dissection. (B) & (B') 2nd week after dissection. (C) & (C') 3rd week after dissection. (D) & (D') 4th week after dissection. (E) & (E') 5th week after dissection. (F) & (F') 6st week after dissection. Arrow shows a cell with a double nucleus during mitosis. (G) & (G') 7th week after dissection. (H) &

(H') 8th week after dissection. (I) & (I') 9th week after dissection. (J) & (J') 10th week after dissection. Scale bar 20 μm. Zoom of lens 20×.

3.1.2 Evaluation of properties of established lepidopteran midgut cell lines (transfectability and spheroids formation)

Transfectability

The purpose of this experiment is the optimization of transfection conditions; i.e. which is the optimal amount of DNA and lipofectin and in which timeframe expression levels are the highest. Three lepidopteran cell lines (AW1 from *H. zea*, Cf203- 900 & Cf1 from *C. fumiferana*) were tested for their transfectability, following transfection with pEIA_EGFP reporter plasmid which expresses GFP under an *Actin* promoter derived from *B. mori*. We tested two conditions for transfection (1st condition: 1 μg DNA & 5 μl lipofectin, 2nd condition: 2 μg DNA & 10 μl lipofectin). As positive control we used Hi5- SF (Fig. 3.3 G- H'), a common insect cell line which is known to be highly transfectable, whereas as a negative control we used the CLG15A cell line (Fig. 3.3 I-J') derived from a hemipteran species (*A. tristis*) where the lepidopteran promoters are expected to be non-functional. The cells were observed under fluorescent microscope 48, 72 and 96 h post transfection.

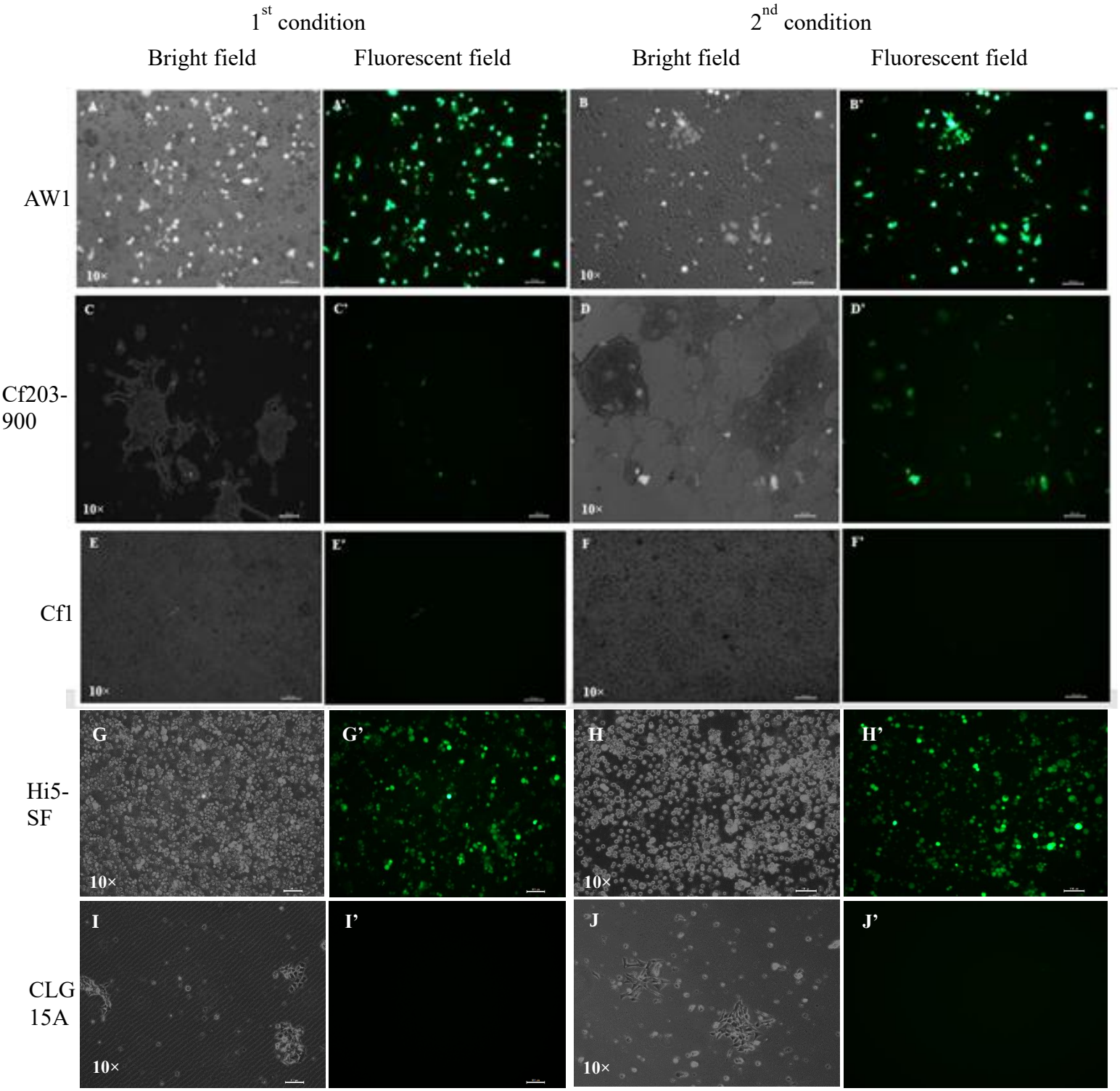

Figure 3.3: Transfectability of established lepidopteran midgut cell lines (AW1, Cf203- 900, Cf1) 72 h post transfection. (A) & (A') AW1 cell line after transfection with 1 µg DNA and 5 µl lipofectin in bright field and fluorescent field, respectively. (B) & (B') AW1 cell line after transfection with 2 µg DNA and 10 µl lipofectin in bright field and fluorescent field, respectively. (C) & (C') Cf203- 900 cell line after transfection with 1 µg DNA and 5 µl lipofectin in bright field and fluorescent field, respectively. (D) & (D') Cf203- 900 cell line after transfection with 2 µg DNA and 10 µl lipofectin in bright field and fluorescent field, respectively. (E) & (E') Cf1 cell line after transfection with 1 µg DNA and 5 µl lipofectin in bright field and fluorescent field, respectively. (F) & (F') Cf1 cell line after transfection with 2 µg DNA and 10 µl lipofectin in bright field and fluorescent field, respectively. (G) & (G') Hi5- SF cell line after transfection with 1 µg DNA and 5 µl lipofectin in bright field and fluorescent field, respectively. (H) & (H') Hi5- SF cell line after transfection with 2 µg DNA and 10 µl lipofectin in bright field and fluorescent field, respectively (positive control). (I) & (I') CLG15A cell line after transfection with 1 µg DNA and 5 µl lipofectin in bright field and fluorescent field, respectively. (J) & (J') CLG15A cell line after transfection with 2 µg DNA and 10 µl lipofectin in bright field and fluorescent field, respectively (negative control). Scale bar 100 µm. Zoom of lens 10×.

As seen in Figure 3.3, each cell line presents different optimal conditions the highest expression was recorded 72 h post- transfection, with small differences between 48 and 96 h post- transfection in AW1 cells. The optimal condition for Cf203- 900 seems to be the 2nd condition (Fig. 3.3 C- D'), whereas both conditions were suitable for AW1 (Fig. 3.3 A- B'). However, for future experiments with AW1 1st condition is preferred. Cf1 cell line is apparently transfectable at an extremely low percentage only at 1st condition (only three positive cells visible), at least with this reporter construct. In our positive and negative controls, we did not observe any differences in any of the two conditions.

Spheroids formation

The two most transfectable cell lines (AW1 and Cf203- 900) were also tested for their ability to form spheroids through the hanging drops method. We performed a hanging-drop protocol as described in 2.5, and after one-week certain 3D structures, were observed as shown in Fig. 3.4. The structures seem to be compact and uniform without bulges. We dissociated the spheroids and we tested with Trypan blue if the cells are alive and no cell death was observed.

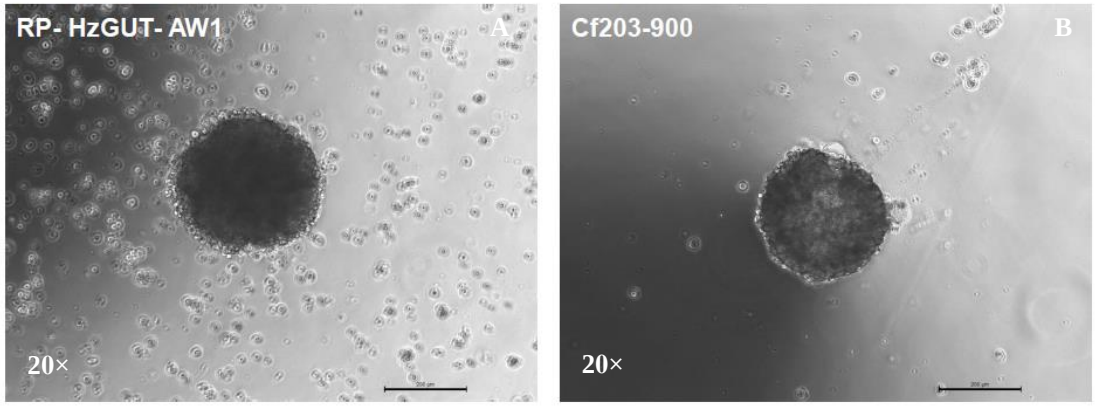

Figure 3.4: Formation of spheroids from AW1 (A) and Cf203- 900 (B) cell lines. Scale bar 200 μm. Zoom of lens 20×.

3.1.3 Selection of candidate marker genes for SSJs and types of midgut cells

20 plates of AW1 cells hanging drops were created for RNA extraction and transcriptomics (five plates for each one of the four replicates). The desirable amount of total RNA was 1 μg for each replicate. Moreover, four replicates of 1 ml non-spheroids AW1 cells were collected for RNA extraction and transcriptomics. All the cells were washed twice with ice- cold 1× PBS before RNA extraction.

In order to determine a set of relevant marker genes that would help us investigate the developmental profile or differentiation status of both primary and established cell lines, as well as investigate the ability of 3D "spheroid" structures to form functional gut-like epithelia bearing SSJs, a series of bioinformatics analyses were performed

(with the valuable help of Shane Denecke) and we validated candidate genes qualitatively by reverse transcription-PCR.

Whole genome sequence of *H. armigera* genome is available (Pearce *et al.*, 2017). Specific genes for the different midgut cell types of *D. melanogaster* midgut (ISCs, ECs and EEs) were selected from the work of Hung *et al.* (2018). We tried to find which of these *Drosophila* genes have 1:1 orthologues (*D. melanogaster*: *H. armigera*) with *H. armigera* midgut specific genes from a previous work in Vontas lab (Panos Ioannidis, unpublished data). We used OrthoDB (https://www.orthodb.org/) for finding the orthologues. From the final list with 1:1 orthologue, 29 genes which were upregulated in larval stages L2, L3 & L4, compared to carcass (using RNAseq information available to the host lab), were chosen (Sup. Table 2). The average midgut expression should be above threshold (mid. Mean of expression > 10 transcripts per million) (Denecke, unpublished data). Then, these genes from *H. armigera* were tested for 1:1 orthology in *H. zea*. Markers for the different midgut cell types (ISCs, ECs, EEs and GCs) were selected manually. Eventually, two to three candidate marker genes for each cell type with the highest mid. mean of expression were selected (Table 3.1).

Table 3.1: Candidate marker genes for SSJs and different types of *Helicoverpa* midgut cells. *Dm*_FBgn: *Drosophila melanogaster* gene code in FlyBase, name: name of *D. melanogaster* gene, *Ha*_og: *Helicoverpa armigera* gene code after blast with *D. melanogaster* gene, annot: name of *H. armigera* gene and hz_og: *H. zea* gene code after blast with *H. armigera* gene.

	***Dm*_FBgn**	**name**	***Ha*_og**	**annot**	***Hz*_og**
Smooth septate junctions (SSJs) markers	FBgn0051004	MESH	HaOG215328	protein mesh	HzOG215328
	FBgn0036945	Ssk	HaOG210831	LOW QUALITY PROTEIN: un protein LOC110372047	HzOG210831
	FBgn0024361	Tsp2A	HaOG210242	tetraspanin-2A	HzOG210242
Intestinal stem cell (ISCs) markers	FBgn0265434	Zip	HaOG211344	myosin heavy chain, non-muscle	HzOG211344
	FBgn0000568	Eip75B	HaOG205019	ecdysone-inducible protein E75	HzOG205019
	FBgn0011674	insc	HaOG213564	uncharacterized protein LOC110373263	HzOG213564
	FBgn0032633	Lrch	HaOG208026	leucine-rich repeat and calponin homology domain-containing protein 2	HzOG208026
	FBgn0004837	Su(H)	HaOG213319	suppressor of hairless protein	HzOG213319

Enterocyte (ECs) markers	FBgn0002522	Lab	HaOG216768	homeotic protein labial-like	HzOG216768
	FBgn0025456	CREG	HaOG213019	protein CREG1	HzOG213019
Enteroendocrine (EEs) markers	FBgn0013343	Syx1A	HaOG212173	syntaxin-1A	HzOG212173
	FBgn0004595	pros	HaOG211128	Homeobox protein prospero	HzOG211128
	FBgn0037976	Tk	HaOG215049	tachykinins-like	HzOG215049

Regarding Goblet cells, which are typical for lepidopteran guts but absent in *Drosophila*, genes encoding for vATPase subunits were used as markers; vATPase proteolipid subunit (HzOG207811) and subunit beta (HzOG206246) (Klein, 1992). As a general reference the gene for elongation factor 1 (EF1) was used. Then, primers for each gene from Table 3.1 were generated and PCR was performed for validation. As it is shown in Fig. 3.5, there is no evident difference between 2D cell culture and spheroids. At this point, no quantitative estimation was performed.

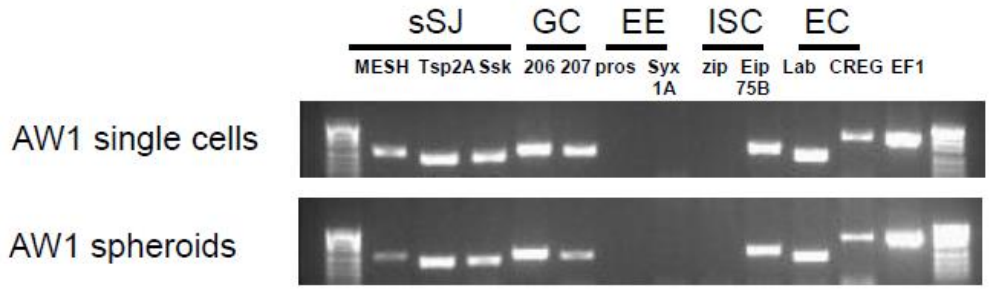

Figure 3.5: Gene expression of AW1 genes in 2D cell culture (AW1 single cells) and spheroids. No difference between cells and spheroids was observed. SSJ: smooth septate junction, GC: Goblet cells, EE: enteroendocrine cells, ISC: intestinal stem cells, EC: enterocytes, 207: vATPase proteolipid subunit and 206: subunit beta.

Smooth septate junction marker genes, enterocyte and Goblet cell are expressed in RP- HzGUT- AW1 (*H. zea*) cells, whereas it seems that only *Eip75B* from ISC markers is expressed (Fig. 3.5). Enteroendocrine markers selected are apparently not expressed. For this reason, we selected some more candidate marker genes for ISCs and EEs to obtain a clearer picture of the AW1 cells expression potential. Hence, we used cDNA and genomic DNA (gDNA) from AW1 and cDNA from *H. armigera* midgut (Fig 3.6). cDNA from *H. armigera* midgut was included to see how conserved are these genes between these two relative species (*H. armigera* and *H. zea*) and check the universality of the primers. This serves also as a kind of positive control.

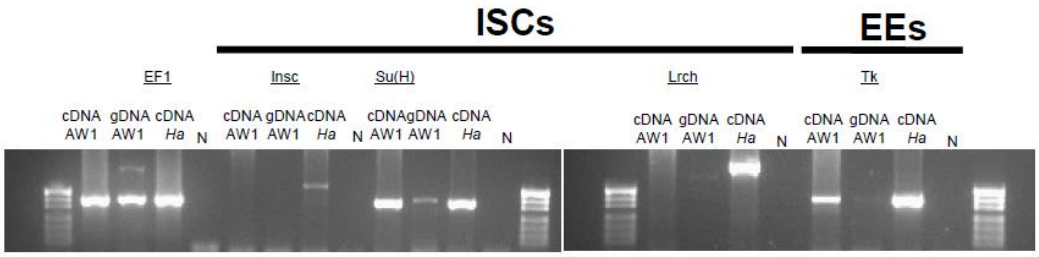

Figure 3. 6: Additional candidate marker genes for AW1 2D culture. ISCs: intestinal stem cells, EEs: enteroendocrine cells. cDNA AW1: cDNA from AW1 cells, gDNA: genomic DNA from AW1 cells, cDNA Ha: cDNA from *Helicoverpa armigera* midgut, N: negative control.

As it is shown in Fig. 3.6, at least one EE marker is expressed. Regarding ISCs again only one (*Su(H)*) of the second set of marker genes is expressed (Fig 3.6). *Su(H)* has been reported as an enteroblast marker (Hung *et al.*, 2018). An overview of expressed and non- expressed markers is summed up in Table 3.4. This whole investigation of candidate marker genes can be used to define "ID" for other differentiated cell lines by creating universal primers for different lepidopteran species and for primary- cell derived cultures. Although the expression pattern is complex and maybe the differentiation of this cell line is incomplete (implicating an arrested differentiation at a point where certain ISC markers are still expressed, while the partly differentiated cells retain the ability to proliferate). The PCR results were qualitative and the number of genes which were tested was limited. Thus, we decided to proceed to transcriptomic analysis that would provide both quantification of gene expression and a complete expression profile of all genes.

Table 3.4: Sum up of expression or not of candidate marker genes for SSJs and types of AW1 cells and *H. armigera* midgut.

	Genes	**RP-HzGUT-AW1**	***H. armigera* midgut**
Smooth septate junctions (SSJs) markers	MESH	+	Unknown
	Ssk	+	Unknown
	Tsp2A	+	Unknown
Intestinal stem cell (ISCs) markers	Zip	-	-
	Eip75B	+	Unknown
	insc	-	-
	Lrch	-	-
	Su(H)	+	+

Enterocyte (ECs) markers	Lab	+	+
	CREG	+	+
Enteroendocrine (EEs) markers	Syx1A	-	-
	pros	-	-
	Tk	+	+
Goblet cell (GCs) markers	vATPase proteolipid subunit	+	+
	Subunit beta	+	+
Reference gene	EF1	+	+

3.1.4 Transcriptomic analysis

3.1.4.1 Differentially expression analysis

First, genes which are differentially expressed between 2D culture and spheroids were examined (analysis performed by Shane Denecke). Then, a table with the genes which are actually differentially expressed was generated (217 genes). So, to manage all these genes and their expression were visualized as a volcano plot (Fig. 3.7). The most upregulated genes in 2D culture encode protein binding factors, calcium binding proteins, ATP binding proteins, actin binding proteins, cell adhesion, nucleic acid binding proteins and plasma membrane proteins, according to GO analysis performed by Shane Denecke. On the other hand, the most upregulated genes in spheroids encode oxidative stress proteins, U5 sRNP, oxidoreductases, imaginal disc- derived wing hair organization proteins and dendrite self- avoidance proteins, according to GO analysis.

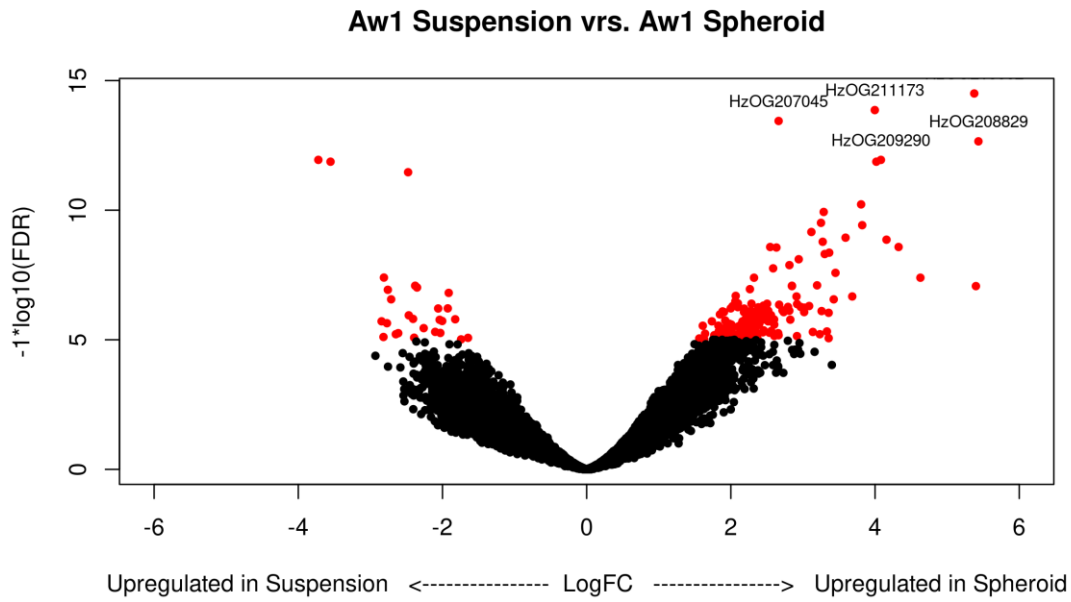

Figure 3.7: Volcano plot representing the differentially expressed genes between single AW1 cells and AW1 spheroids. The y axis represents the false discovery rate (FDR) and the x axis the log fold change (logFC). The red dots show genes which are below FDR threshold, whereas black dots non- significant. In the negative side are located the upregulated genes in 2D cell culture samples and in the positive side the upregulated genes in spheroids samples (Denecke, unpublished data).

3.1.4.2 Analysis of candidate cell type marker genes

The extended candidate marker genes which were used in section 3.1.3., were considered in AW1 2D culture. A dot plot was generated (Fig. 3.8), where the genes of different midgut cell types from Sup. Table 2 categorized to each cell type (EC, ISC & EE) and depicted according to their expression levels from transcriptomics. The markers from no one of the cell types seem to be upregulated compared to others, so we cannot say in which cell type AW1 cell line belongs, if it can be readily attested to any specific type.

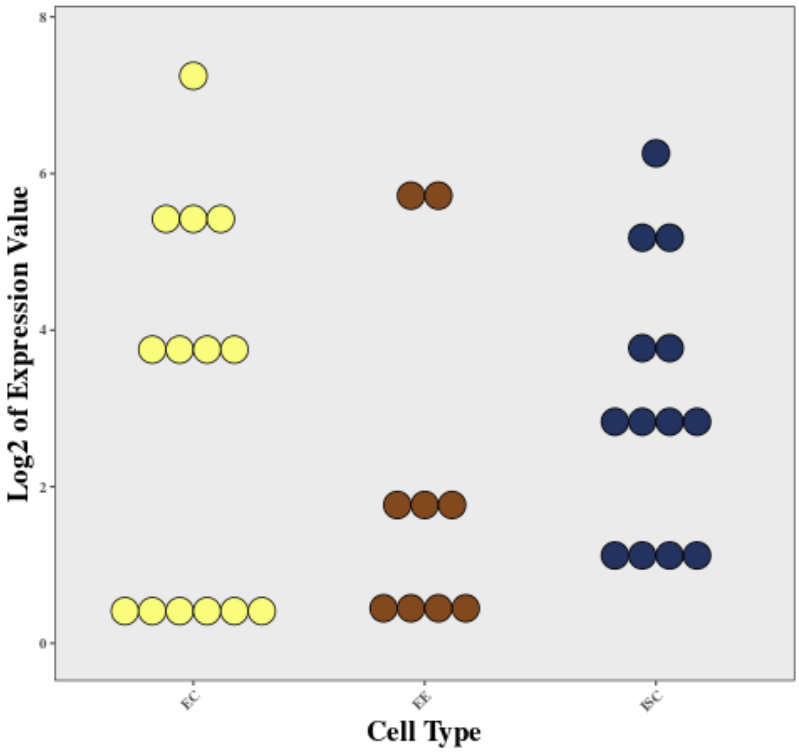

Figure 3.8: Marker genes from section 3.1.3 divided by cell type and plotted according to their expression levels in single AW1 cells. Expression levels of different midgut cell type marker genes in AW1 2D culture. Each dot represents one gene. The y axis represents the log2 of expression value and the x axis the different cell types. EC: enterocyte, EE: enteroendocrine cell, ISC: intestinal stem cell (Denecke, unpublished data).

3.1.4.3 Analysis of candidate sSJ marker genes

In order to further investigate the spheroids, we chose to focus on componnets of sSJ to see if they are differentially expressed. Except the three main sSJ marker genes (*Mesh*, *Ssk* and *Tsp2A*), more marker genes for sSJ were used. Out of the 46 genes from the sSJ GO term, the total number of marker genes identified in *H. zea* was 40. In addition, a plot (Fig. 3.9) for these data was created which displays the fold change in each sSJ gene in spheroids compared to non-spheroids (2D culture). The sSJ marker genes appear to be slightly upregulated in non- spheroid cells compared to spheroid. This suggests the opposite of the initial hypothesis that spheroids have an increase in sSJ expression. Hence, our results do not support the initial hypothesis that these spheroids are an organized system.

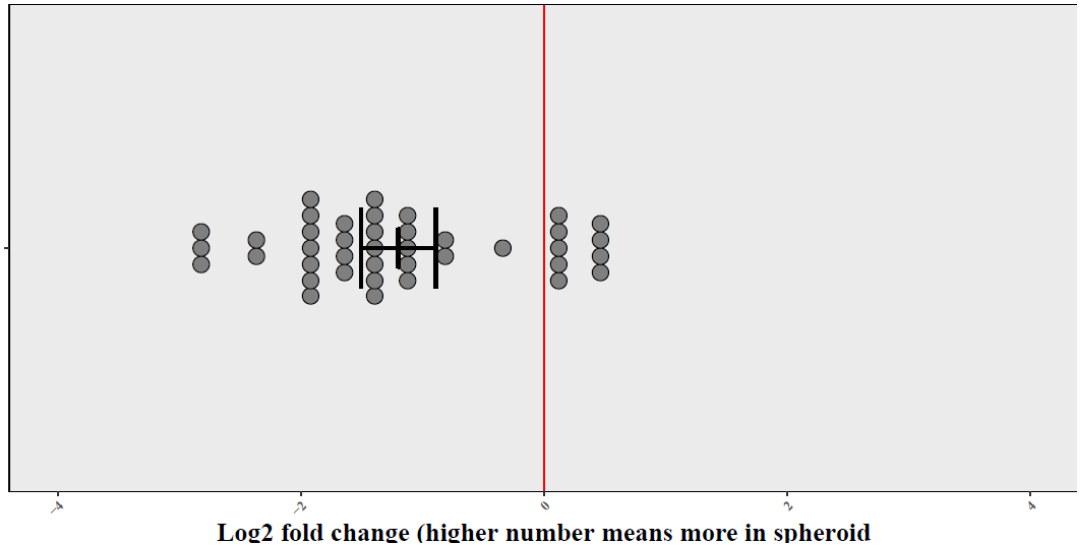

Figure 3.9: Plotting expression of SSJ genes. The red line indicates zero. Left: the enriched SSJ marker genes in 2D culture. Right: the enriched SSJ marker genes in spheroids. Each circle represents one gene. This plot has only one axis. The plot is divided in two parts by a red line which indicates no difference between the two samples (zero). The left part of the graph indicates the enriched genes in single 2D culture whereas the right part indicates highly expressed SSJ genes in spheroids. Each circle represents one gene and most of the genes are in the left part of the plot (Denecke, unpublished data).

All the analyses and the figures of section 3.1.4 were generated by Dr Shane Denecke.

3.2 Validation of target-site resistance mutation I310T via CRISPR/Cas9 in *Drosophila*

The purpose of this study is to functionally validate the I310T alteration in the *GluCl* gene in resistance against abamectin by performing genome engineering using *Drosophila melanogaster* as a model organism. The achievement of establishing a fly strain population for this mutation in this particular gene is really important because CRISPR/Cas9 is difficult to be performed in *T. urticae* and previous studies in Vontas lab have shown that other alterations in the same region of this gene are lethal in *Drosophila* (Iason Chistou, MSc thesis).

3.2.1 CRISPR mediated substitution of I310T in *Drosophila melanogaster*

Our strategy was to create modified flies that carry mutation I310T in the *Drosophila GluCl* gene and finally to validate and elucidate its actual contribution to the resistance to abamectin. The whole amino acid sequence of *GluCl* gene was obtained from 11 different insect species by using NCBI site (*T. urticae, P. xylostella, Apis mellifera, Musca domestica, D. melanogaster, Tribolium castaneum*, etc) and from the five *GluCl* genes which existed in *T. urticae* and were aligned with Clustal Omega (1.2.4). EMBL-EBI (Fig. 1.2) (Papapostolou and Vontas, unpublished data). The orthologue *GluCl* gene in *Drosophila* was found and based on the alignment the target region was identified in order to design the strategy to obtain the mutation under study (Fig. 2.2).

The CRISPR/Cas9 genome modification was performed as described (see 2.8). For the I310T mutation, 27 G_0 adult flies were backcrossed with nos.Cas9 strain and 9 out of them were sterile. The G_1 progeny of the remaining 18 was screened with either "specific" primers or digestion after amplification with generic primers as described in 2.10. Five out of the 18 crosses were found to give progeny positive for the HDR (Fig. 3.10).

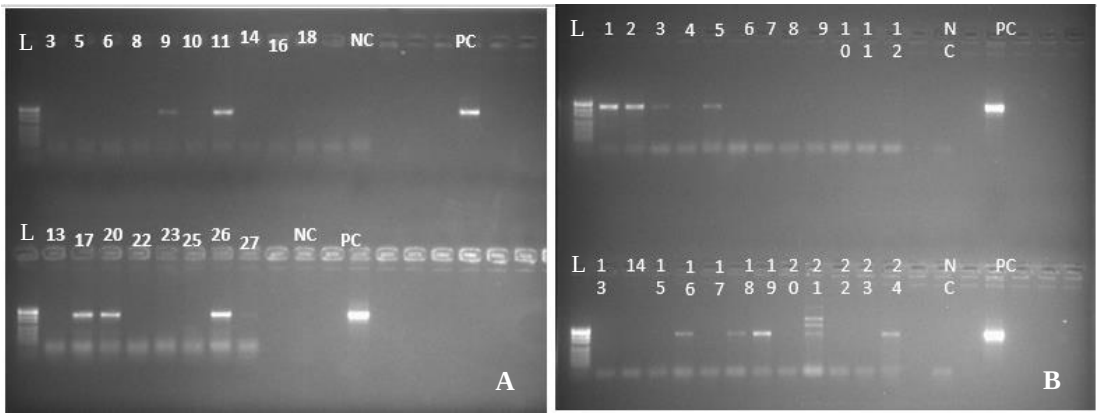

Figure 3.10*:* Diagnostic screening with specific primers yielding a 489 bp product running in 2% agarose gel. L (Puc19/ BsisI) indicates the MW ladder while PC indicates the positive control (donor plasmid used for the mutation) used for the experiments, NC indicates the negative control of the experiment which was the non-injected nos. Cas9 gDNA. (A) PCR screening with specific primers (489 bp) of G_1 pupae pools, progeny from G_0 lines injected nos- Cas9 with uninjected nos- Cas9 (background strain). (B) PCR screening with specific primers (489 bp) of G_1 individuals originating from each original line (G_0) for the mutation crossed with balancer TM3/ TM6B.

G_1 individuals originating from the original positive lines (G_0) were crossed with nos.Cas9 adults and they were then screened in order to identify positive heterozygotes. The screening in individual adults was performed with PCR using "specific" primers (see Sup. Table 1), which yields a fragment of 489 bp, as it is depicted in Figure 3.10. G_2 progeny from the crosses containing a G_1 positive parent were crossed with balancer flies for the third chromosome and molecular screening was carried out in order to distinguish the crosses that came from positive G_2 flies. After the final crosses in order to obtain homozygous modified flies, two lines (IT9.8 & IT11.6) for the mutation were established. Both lines were checked by sequencing in order to verify that HDR mechanism worked successfully which is depicted in figure 3.11. The strain population seems to develop slowly, which could indicate some fitness cost associated with the mutation. Downstream experiments concerning toxicity bioassays against abamectin, are needed in order to study the contribution of this mutation to resistance (work in progress).

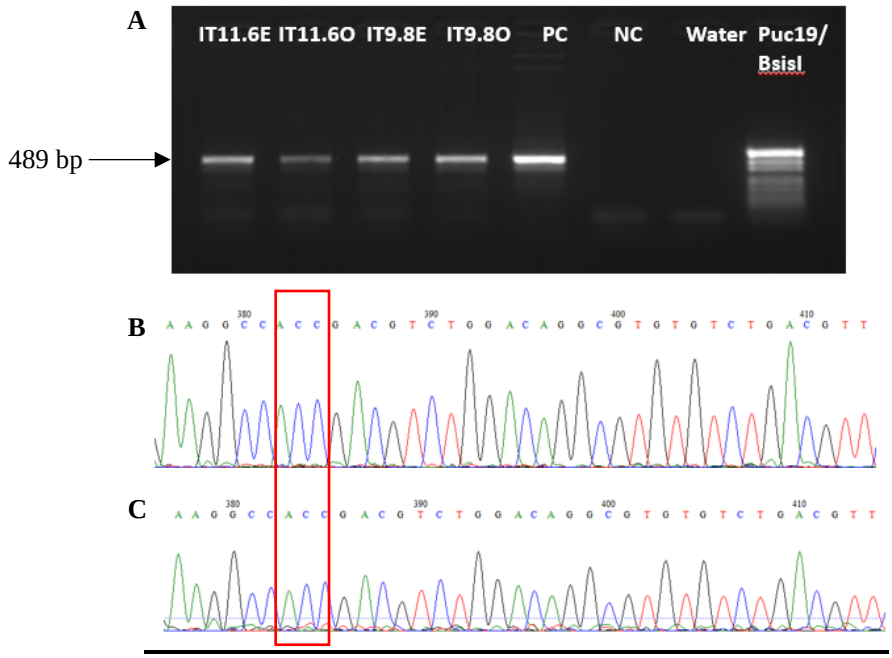

Figure 3.11: PCR with generic primers (A) of homozygous lines (IT11.6O & IT9.8O) and heterozygous lines (IT11.6E 7 IT11.6O). Chromatograms of the sequencing results of homozygous lines established for each mutation. (B) For homozygous line IT11.6 & (C) for homozygous line 9.8. I310T amino acids are indicated with red frame. PC: positive control, NC: negative control, Water: PCR mix without DNA, Puc19/ BsisI: ladder.

3.3 Functional expression of P450 detoxification genes with baculovirus

The objective of this study is to functionally express three P450s from *Apis mellifera* (CYP9Q1, CYP9Q2 and CYP9Q3) in Sf9 cells by employing the baculovirus expression system. These three P450 expressing viruses were used for co- infection and finally co- expression with *Anopheles gambiae* CPR in Sf9 cells. Furthermore, they were functionally validated via CO-spectrum and CPR assay. Then, microsomes containing these protein complexes were generated and can be used for downstream experiments for checking *in vitro* model substrate and insecticide detoxification.

3.3.1 Generation and amplification of recombinant baculoviruses for *Apis mellifera* P450s (CYP9Q1, CYP9Q2 and CYP9Q3) and *Anopheles gambiae* CPR (AgCPR)

Following BACmid transfection in Sf9 cells and generation of relevant viruses, the concentration of CYP9Q1 was 7×10^7 FFU/ml whereas the concentrations of CYP9Q2, CYP9Q3 and CPR were approximately 4×10^7 FFU/ml.

Infected cells were used for Western analysis. (Fig. 3.12). The blots confirm the expression of all P450s of as well as AgCPR at the predicted molecular weight (AgCPR: 77.2 kDa, CYP9Q1: 58.8 kDa, CYP9Q2: 60.9 and CYP9Q3: 58.8). P450s are tagged with a 6xHis- tag. For the P450s we used anti-His antibody, while for the AgCPR we used an anti-CPR antibody (this protein is not tagged).

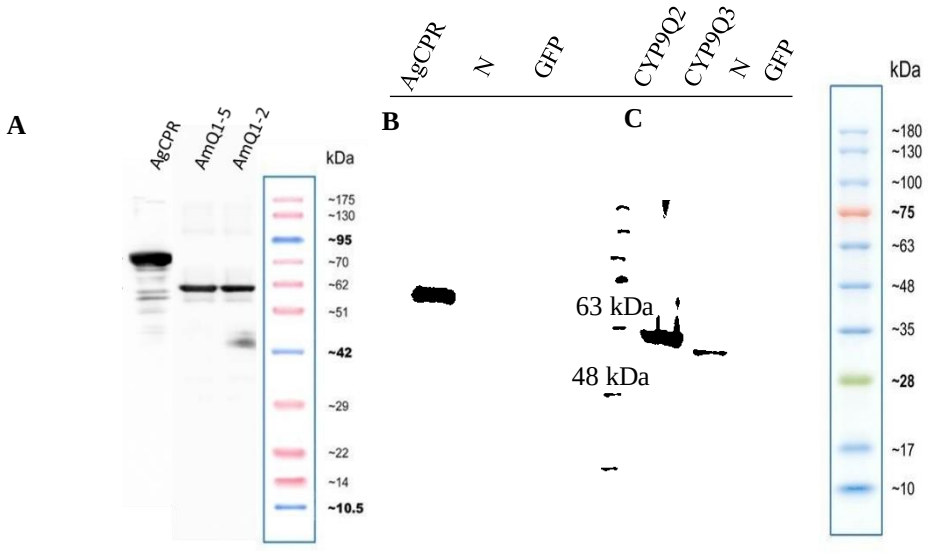

Figure 3.12: Western blot analysis for AgCPR and CYP9Q1-3 expressed in baculovirus. (A) AgCPR (77.2 kDa) and two different AmQ1 (CYP9Q1) (58.8 kDa) clones, (B) AgCPR and (C) CYP9Q2 (60.9 kDa) & CYP9Q3 (58.8 kDa). N: negative (no virus), G: GFP virus. The results indicate that both AgCPR and bee P450s are expressed in baculovirus infected insect cells.

3.3.2 Functional validation of microsomal proteins after co- expression of bee P450s and AgCPR

Regarding functional validation of bee P450s and CPR (10:1) co- expression, CO spectrum assay and CPR activity assay were performed. As seen in Table 3.5, a P450 peak at CYP9Q1, CYO9Q2 and CYP9Q3 was detected. It seems that all P450s have the ability to convert the Fe of heme to reducing Fe after the addition of CO gas and sodium hydrosulfite (reducing agent). As monooxygenases, P450s catalyze the transfer of one atom of molecular oxygen to a substrate and reduce the other to water. The best CO-spectrum with the clearest peak is in CYP9Q2 protein. All the samples have also CPR activity from the estimated velocity.

Table 3.5: Baculovirus expression data for CYP9Q1, CYP9Q2 and CYP9Q3 microsomal proteins at 10 P450: 1 CPR virus infection ratio. The red square points out the peaks at 450 nm for P450s. Table is created by Dimitra Tsakireli.

A/A	Sample Name	Sample details of molar ratio p450 :CPR	Figure of CO Spectrum	Content of P450 uM	CPR activity nmol/min/mgr
1	Negative Control	SF9 cells with a BACmid containing a GFP-Myc tagged ORF	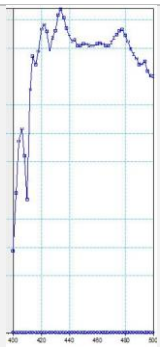	No peak	No activity
2	CYP9Q1 10:1	10 baculovirus with p450 Q1 : 1 baculovirus with CPR	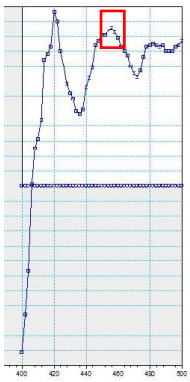	2.46	90.87
3	CYP9Q2 10:1	10 baculovirus with p450 Q2 : 1 baculovirus with CPR	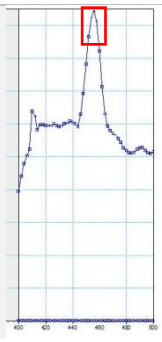	16	73.57
4	CYP9Q3 10:1	10 baculovirus with p450 Q3 : 1 baculovirus with CPR	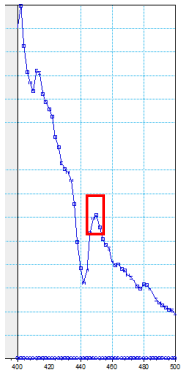	25.7	81.41

4. Discussion and conclusions

4.1 Insect cell based assays for drug discovery

4.1.1 Primary midgut cell culture of *Helicoverpa armigera* is feasible to generate, and holds promise for development of stably differentiated midgut lines

In this study, we applied different protocols towards the generation of primary midgut cell line from *H. armigera*. Three different protocols were used according to literature (Loeb *et al.,* 2003; Cermenati *et al.,* 2007; Li *et al.,* 2015). The first effort was based in Li *et al.* (2015) protocol, where they generated a primary midgut cell line from *H. armigera* fourth instar larvae. From the 60 cultures they had generated, only one grew gradually. They let this one culture to grow until two months and then they subcultured it every four to six days (Li *et al.,* 2015). The cell line mostly consisted of ISCs and not GCs and ECs, because these two differentiated cell types cannot proliferate. Regarding their morphology features they were 13.8± 1.8 μm in diameter. The proliferation rate was 58.6± 7.0 h at 28^{o} C (Li *et al.,* 2015). They performed also several tests: transfectability, chromosome analysis, cells permissiveness to *Autophaga californica* nuclear polyhedrosis virus and *H. armigera* nuclear polyhedrosis virus, susceptibility to Cry toxins and proliferation induction by 20- Hydroxyecdysterone (Li *et al.,* 2015). Unfortunately, our effort based on this protocol was not successful, since the cells survived for eight weeks without any visible proliferation.

Thus, we tried to incorporate some changes in this initial protocol from Loeb *et al.* (2003) and Cermenati *et al.* (2007). In both of these papers they use strainers. After these changes our cell line survived for 10 weeks and started to proliferate around fourth week. Both papers report the generation of midgut cell lines from two different lepidopteran species *Heliothis virescens* (Loeb *et al.,* 2003) and *Bombyx mori* (Cermenati *et al.,* 2007). Cermenati *et al.* (2007) reported that stem cells were round with 4- 8 μm diameter (Fig 4.1). Early ECs and GCs were 25- 30 μm in diameter and had their characteristics shapes: square- shaped with microvilli for ECs and pear-shaped for GCs (Fig 4.1). The cultured ECs and GCs were smaller than the cells which exist in midgut epithelium (60- 80 μm diameter). ISCs proliferated and differentiated to ECs after three weeks which were used for downstream experiments. These cells kept their functional properties until 42nd day (Cermenati *et al.,* 2007).

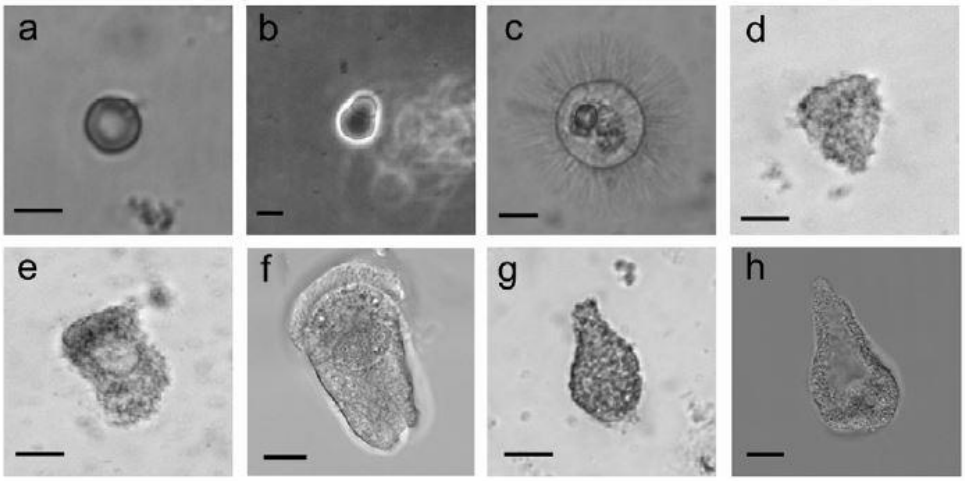

Figure 4.1: Cell types as are depicted in Cermenati *et al.*, 2007. (a) ISC, (b) proliferating ISC, (c) & (d) differentiating cells, (e) early EC, (f) mature EC (g) early GC, (h) mature GC (Cermenati *et al.*, 2007).

We observed, also, cell aggregates as obtained in previous works (Loeb *et al.*, 2003; Cermenati *et al.*, 2007; Li *et al.*, 2015). We added conditioned medium from an available midgut insect cell line (AW1) to provide growth factors that may induce proliferation and differentiation, since various factors produced by mature and differentiating cells assist this (Loeb *et al.*, 2004). Future plans for this work includes performing certain tests Li *et al*. (2015) have done. Furthermore, we need to verify that the cell types growing are indeed gut derived, to use differentiation factors in order to induce differentiation of ISCs and if a line is established to investigate if they form monolayers and spheroids for testing different chemical compounds. Known cell multiplication factors include 20- Hydroxyecdysterone, which maintains stem cell proliferation in culture, A- arylophorin, which promotes stem cell mitosis, and Bombyxin, that increases around 40% the stem cell number (Loeb 2010). On the other hand, certain midgut differentiation factors that can be tested are peptides MDF1 (HVGKTPIVGQPSIPGGPVRLCPGRIR), which promotes maximum differentiation of *H. virescens* larval-type stem cells, MDF2 (HRAHY), which can induce around 58% of about 3000 newly differentiated cells to become columnar-like, MDF3 (EEVVKNAIA) and MDF4 (ITPTSSLAT), which are very active in inducing 4th instar-like differentiation of *H. virescens* midgut stem cells (Loeb and Jaffe 2002).

4.1.2 Established lepidopteran midgut cell lines are transfectable and have the ability to for spheroid-like structures

After transfection with pEIA_EGFP plasmid, AW1 and Cf203- 900 midgut cell lines were fluorescent. The *EGFP* gene is regulated by an *Actin* promoter from *Bombyx mori*, which is expressed ubiquitously among tissues of lepidopteran species. The transfectability property of these midgut specific cell lines was used to express *EGFP* gene under the control of other promoters which were isolated from midgut specific genes (Samantsidis and Denecke, unpublished data). Two promoters from *H. armigera* midgut specific genes were tested: *APN1(aminopeptidase 1)* promoter (Jiang *et al.*, 2015) and *mucin* promoter (Campbell *et al.*, 2008). AW1 cells which were transfected

with *EGFP* expressing plasmid under *mucin* promoter were fluorescent, whereas the ones under *APN1* promoter were not. Furthermore, Cf203- 900 cells were not fluorescent for any of the two promoters (Samantsidis, unpublished data).

In addition, AW1 and Cf203- 900 were tested for their ability to form spheroids and apparently they form rigid 3D structures resembling spheroids. These spheroids could be used for downstream experiments in order to test if various compounds use the paracellular diffusion. To further investigate their properties, we performed RNAseq analysis for spheroids from the AW1 cell line to gain insight to their expression profile and see if the sSJs markers (*MESH, Tsp2A, Ssk* and others) are upregulated compared to conventional 2D cultures.

We performed a series of experiments trying to tackle two questions:1) Do AW1 cells resemble the differentiation profile of a specific midgut cell type? and 2) Do the AW1 spheroids form sSJs, i.e. do they form an epithelium similar to the midgut? In order to answer these two questions, we performed a series of bioinformatics analyses, PCRs and transcriptomics. Regarding to first question transcriptomics analysis did not provide a definite answer. None of the different midgut cell type markers were more upregulated than the others. This probably indicates that AW1 cells are only partially differentiated and more related to enteroblasts (EBs) (Fig 4.2), which come from ISCs proliferation and are ECs and EEs progenitors (Hung *et al.*, 2018). We are not able to further characterize these cells at this point, although the RNAseq dataset provides a starting point for future research. Probably further analysis and experiments are required, involving perhaps single-cell RNAseq approaches.

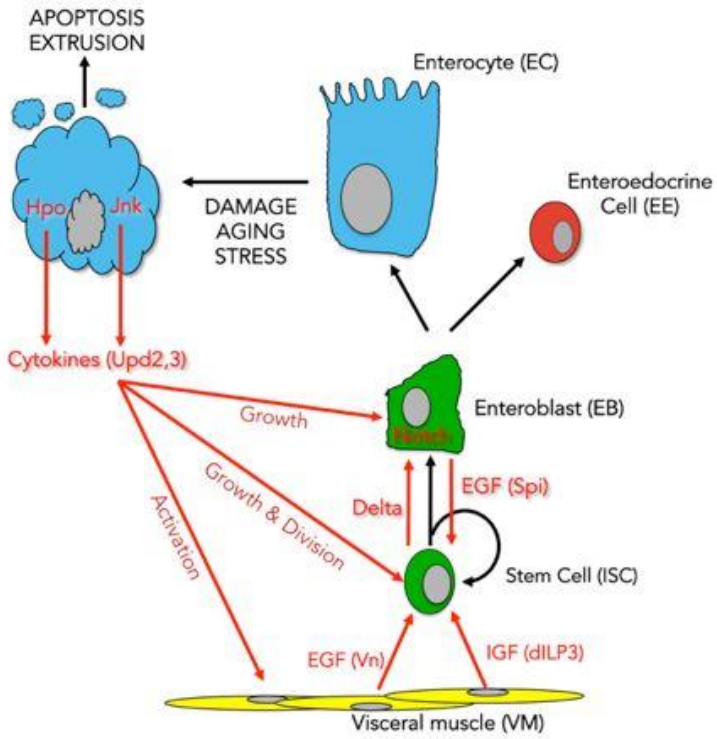

Figure 4.2: Figure from Edgar lab site. Model explaining epithelial renewal in the *Drosophila melanogaster* midgut. Cell linage depicted with black arrows, cell signaling interactions depicted with red. (https://uofuhealth.utah.edu/huntsman/labs/edgar/research.php)

Regarding the second question we can see from Fig. 3.7 that the upregulated genes in spheroids and non- spheroids are different. So, they are indeed two different states with a different expression profile. Furthermore, the most upregulated genes in spheroids belong to oxidative stress related genes, which indicates that spheroids are a stressful state for the cells. We aimed to investigate if the spheroids form sSJs, i.e. that they are an organized system. If this was true, one could perform downstream experiments to test the paracellular diffusion. An interesting technique has been reported to measure transepithelial/ transendothelial electrical resistance of tight junctions in mammalian endothelial and epithelial cell monolayers (Srinivasan *et al.,* 2015). This technique indicated the integrity of cellular barriers and it can be used before the evaluation of chemical compounds such as drugs (Srinivasan *et al.,* 2015). Efforts to measure septate junction permeability and investigate the paracellular pathway have been reported in *Bombyx mori* (Fiandra *et al.,* 2005). However, no sSJ gene upregulation was observed, thus the initial hypothesis was not confirmed, and these spheroids seem to be little more than cell clumps. However, downstream experiments of adding differentiation factors to spheroids to test if they differentiate to ECs and form sSJ could be performed and then test pigments and other compounds. Spheroids were considered an alternative to Caco- 2 assay for testing midgut permeability in different compounds, since the insect cell lines cannot form a permanent monolayer. Downstream experiments, also, might include immunolocalization of sSJs in spheroids. Unfortunately, there are no available antibodies for *Helicoverpa sp*.

Although the transcriptomics data could not support the initial hypotheses, transcriptome of *H. zea* midgut cell line AW1 is definitely a useful tool, to understand more properties of these cells and to use it for manipulations and for comparisons with other midgut cell lines derived from lepidopteran species.

4.2 Validation of target-site resistance mutation I310T by CRISPR/Cas9 in *Drosophila*

IT11.6 is the first *Drosophila melanogaster* strain in our lab that carries in homozygous situation a mutation (I310T) in *glutamate gated chloride channel* (*GluCl*) gene. This mutation has been first reported in *GluCl3* of *Tetranychus urticae* (Papapostolou and Vontas, unpublished data). Flies with other mutations in the same region of *GluCl* from previous work in the lab (Christou and Douris, unpublished data) could only have the mutation in heterozygous state.

Several mutations in glutamate gated chloride channel subunits in *T. urticae* have been associated with resistance in abamectin. G314D in GluCl and G326E in GluCl3 in *T. urticae* have been previously reported that confer to abamectin resistance > 2000 fold (Dermauw *et al.,* 2012). Mutation G326E was also validated functionally in *Xenopus* oocytes using two- electrode clamp electrophysiology which proved that this mutation confers resistance to abamectin and that GluCl3 is a molecular target of abamectin (Mermans *et al.,* 2017). In addition, Kwon *et al.* (2010) identified in GluCl1 of *T. urticae* a G323D point mutation which is tightly associated with a moderate resistance

phenotype (17- fold resistance). Resistant mutations in *GluCl* genes in other invertebrates have been also reported. Some examples are P299S in *D. melanogaster* correlated with ivermectin resistance (Kane *et al.,* 2000), E114G, V235A and L256F in GluCla3 and V60A and R101H in GluClb of nematode *Cooperia onchophora*, with abamectin resistance (Njue *et al*., 2004). Furthermore, GluCl channels may also play a secondary role in mediating toxicity of other insecticides (e.g. fipronil), as this has been documented in German cockroaches (Narahashi *et al*., 2010).

Regarding the I310T mutation, it has been associated with abamectin resistance. It has already been validated with two- electrode clamp electrophysiology in *Xenopus* oocytes (Van Leeuwen, personal communication). At the same time genetic crosses of *T. urticae* are performed in order to conclude in a strain which bears the I310T mutation in homozygous state (Skoufa and Vontas, personal communication). This strain, which has the same genetic background with the susceptible one except the I310T mutation, will be used later for bioassays with abamectin.

Future work in *Drosophila* includes expansion of the homozygous strain and bioassays with abamectin and probably other avermectin insecticides. Finally, detailed assays to investigate if there is any fitness cost associated with the mutation are required, since is observed that the emergence of adults is three days delayed compared to the original unmodified strain of the same genetic background. These experiments are currently in progress.

4.3 Functional expression of honeybee P450 detoxification genes with baculovirus

We achieved to express *Apis mellifera* P450s (CYP9Q1, CYP9Q2 & CYP9Q3) via heterologous expression through the baculovirus system in Sf9 cells. Moreover, these proteins were shown to be functional. Several studies have used baculovirus expression system in insect cells for insect P450s expression. *Drosophila* CYP6A2 has also been expressed with baculovirus (Feyereisen, 2012). The co- infection of reductase with P450s has improved the system's efficacy (Feyereisen, 2012). For example, the activity of CYP6B1 against xanthotoxin was raised after the co infection (Feyereisen, 2012). Gong *et al.* (2017) co- expressed two *Culex* mosquitoes P450s genes, *CYP9M10* and *CYP6AA,* with cytochrome P450 reductase in Sf9 cells, in order to show their important role in permethrin (insecticide) and its metabolites, PBOH and PBCHO, detoxification. Another improvement is the addition of hemin in culture medium for increased P450s production (Wen *et al.,* 2003).

A great advantage of baculovirus system is that P450s purification is not necessary, since they are expressed in insect cell membranes (ER and mitochondrial membranes), i.e their natural subcellular localization. There are some advantages in baculovirus expression system in comparison to *E. coli* heterologous P450s expression system. In the baculovirus system, it is important to define the optimal P450/ P450 reductase ratio for the highest cell lysate

activity, whereas in *E. coli* expression system the P450 quantity is important. (Feyereisen, 2012). Usually the expression level of endogenous P450s is minor in the cells (e.g. Sf9), however maybe it should be taken into consideration when activity measurements are pretty low. Slight modifications of P450s could help even these which are poorly expressed with baculovirus system to express properly. In conclusion, the baculovirus expression system is one of the most appropriate systems for functional expression of insect P450s, since it is the least heterologous among available systems.

5. References

Balabanidou, V., A. Kampouraki, M. MacLean, G. J. Blomquist, C. Tittiger, M. P. Juarez, S. J. Mijailovsky, G. Chalepakis, A. Anthousi, A. Lynd, S. Antoine, J. Hemingway, H. Ranson, G. J. Lycett and J. Vontas (2016). "Cytochrome P450 associated with insecticide resistance catalyzes cuticular hydrocarbon production in Anopheles gambiae." Proc Natl Acad Sci U S A **113**(33): 9268-9273.

Bassett, A. R., C. Tibbit, C. P. Ponting and J. L. Liu (2013). "Highly efficient targeted mutagenesis of Drosophila with the CRISPR/Cas9 system." Cell Rep **4**(1): 220-228.

Brown, M. A., L. O. Ruzo and J. E. Casida (1986). "Photochemical conversion of a dicofol impurity, alpha-chloro-DDT, to DDE." Bull Environ Contam Toxicol **37**(6): 791-796.

Campbell, P. M., A. T. Cao, E. R. Hines, P. D. East and K. H. Gordon (2008). "Proteomic analysis of the peritrophic matrix from the gut of the caterpillar, Helicoverpa armigera." Insect Biochem Mol Biol **38**(10): 950-958.

Casida, J. E. and K. A. Durkin (2013). "Neuroactive insecticides: targets, selectivity, resistance, and secondary effects." Annu Rev Entomol **58**: 99-117.

Chattopadhyay, P., G. Banerjee and S. Mukherjee (2017). "Recent trends of modern bacterial insecticides for pest control practice in integrated crop management system." 3 Biotech **7**(1): 60.

Cermenati, G., P. Corti, S. Caccia, B. Giordana, M. Casartelli (2007). "A morphological and functional characterization of *Bombyx mori* larval midgut cell in culture". Research report

Daborn, P. J., J. L. Yen, M. R. Bogwitz, G. Le Goff, E. Feil, S. Jeffers, N. Tijet, T. Perry, D. Heckel, P. Batterham, R. Feyereisen, T. G. Wilson and R. H. ffrench-Constant (2002). "A single p450 allele associated with insecticide resistance in Drosophila." Science **297**(5590): 2253-2256.

Dahanukar, A. and R. P. Wharton (1996). "The Nanos gradient in Drosophila embryos is generated by translational regulation." Genes Dev **10**(20): 2610-2620.

Denecke, S., L. Swevers, V. Douris and J. Vontas (2018). "How do oral insecticidal compounds cross the insect midgut epithelium?" Insect Biochem Mol Biol **103**: 22-35.

Dermauw, W., A. Ilias, M. Riga, A. Tsagkarakou, M. Grbic, L. Tirry, T. Van Leeuwen and J. Vontas (2012). "The cys-loop ligand-gated ion channel gene family of Tetranychus urticae: implications for acaricide toxicology and a novel mutation associated with abamectin resistance." Insect Biochem Mol Biol **42**(7): 455-465.

Douris, V., K. M. Papapostolou, A. Ilias, E. Roditakis, S. Kounadi, M. Riga, R. Nauen and J. Vontas (2017). "Investigation of the contribution of RyR target-site mutations in diamide

resistance by CRISPR/Cas9 genome modification in Drosophila." Insect Biochem Mol Biol **87**: 127-135.

Douris, V., D. Steinbach, R. Panteleri, I. Livadaras, J. A. Pickett, T. Van Leeuwen, R. Nauen and J. Vontas (2016). "Resistance mutation conserved between insects and mites unravels the benzoylurea insecticide mode of action on chitin biosynthesis." Proc Natl Acad Sci U S A **113**(51): 14692-14697.

Douris, V., L. Swevers, V. Labropoulou, E. Andronopoulou, Z. Georgoussi and K. Iatrou (2006). "Stably transformed insect cell lines: Tools for expression of secreted and membrane-anchored proteins and high- throughput screening platforms for drug and insecticide discovery". Adv Virus Res **68**: 113- 156

Edmondson, R., J. J. Broglie, A. F. Adcock and L. Yang (2014). "Three-dimensional cell culture systems and their applications in drug discovery and cell-based biosensors." Assay Drug Dev Technol **12**(4): 207-218.

Ffrench- Constant, R. H. (2013). "The molecular genetics of insecticide resistance". Genetics **194**(4): 807-15.

Fiandra, L., M. Casartelli and B. Giordana (2006). "The paracellular pathway in the lepidopteran larval midgut: modulation by intracellular mediators." Comp Biochem Physiol A Mol Integr Physiol **144**(4): 464-473.

Feyereisen, R (2012). "Insect CYP genes and P450 Enzymes" **8**: 236- 295

Furuse, M. and Y. Izumi (2017). "Molecular dissection of smooth septate junctions: understanding their roles in arthropod physiology." Ann N Y Acad Sci **1397**(1): 17-24.

Gong, Y., T. Li, Y. Feng and N. Liu (2017). "The function of two P450s, CYP9M10 and CYP6AA7, in the permethrin resistance of Culex quinquefasciatus." Sci Rep **7**(1): 587.

Gratz, S. J., A. M. Cummings, J. N. Nguyen, D. C. Hamm, L. K. Donohue, M. M. Harrison, J. Wildonger and K. M. O'Connor-Giles (2013). "Genome engineering of Drosophila with the CRISPR RNA-guided Cas9 nuclease." Genetics **194**(4): 1029-1035.

Gratz, S. J., F. P. Ukken, C. D. Rubinstein, G. Thiede, L. K. Donohue, A. M. Cummings and K. M. O'Connor-Giles (2014). "Highly specific and efficient CRISPR/Cas9-catalyzed homology-directed repair in Drosophila." Genetics **196**(4): 961-971.

Homem. R. A. and T. G. E. Davies (2018)."An overview of functional genomic tools in deciphering insecticide resistance." Curr Opin Insect Sci **27**: 103-110

Hung, R. J., Y. Hu, R. Kirchner, F. Li, C. Xu, A. Comjean, S. G. Tattikota, W. R. Song, S. H. Sui and N. Perrimon (2018). "A cell atlas of the adult *Drosophila* midgut". bioRxiV

Izumi, Y., Y. Yanagihashi and M. Furuse (2012). "A novel protein complex, Mesh-Ssk, is required for septate junction formation in the Drosophila midgut." J Cell Sci **125**(Pt 20): 4923-4933.

Jiang, H., P.H. Patel, A. Kohlmaier, M.O. Grenley, D.G. McEwen, and B.A.Edgar (2009). "Cytokine/Jak/Stat signaling mediates regeneration and homeostasis in the Drosophila midgut". Cell **137**: 1343-1355.

Jiang, H., M.O. Grenley, M.J. Bravo, R.Z. Blumhagen, and B.A. Edgar (2011). "EGFR/Ras/MAPK signalingmediates adult midgut epithelial homeostasis and regeneration in Drosophila". Cell Stem Cell **8**: 84-95.

Jiang, L., C. Huang, Q. Sun, H. Guo, T. Cheng, Z. Peng, Y. Dang, W. Liu, G. Xu and Q. Xia (2015). "The 5'-UTR intron of the midgut-specific BmAPN4 gene affects the level and location of expression in transgenic silkworms." Insect Biochem Mol Biol **63**: 1-6.

Jinek, M., K. Chylinski, I. Fonfara, M. Hauer, J. A. Doudna and E. Charpentier (2012). "A programmable dual-RNA-guided DNA endonuclease in adaptive bacterial immuntiy". Science **337**(6096): 816-21

Kane, N. S., B. Hirschberg, S. Qian, D. Hunt, B. Thomas, R. Brochu, S. W. Ludmerer, Y. Zheng, M. Smith, J. P. Arena, C. J. Cohen, D. Schmatz, J. Warmke and D. F. Cully (2000). "Drug-resistant Drosophila indicate glutamate-gated chloride channels are targets for the antiparasitics nodulisporic acid and ivermectin." Proc Natl Acad Sci U S A **97**(25): 13949-13954.

Klein, U. (1992). "THE INSECT V-ATPase, A PLASMA MEMBRANE PROTON PUMP ENERGIZING SECONDARY ACTIVE TRANSPORT: IMMUNOLOGICAL EVIDENCE FOR THE OCCURRENCE OF A V-ATPase IN INSECT ION-TRANSPORTING EPITHELIA." J Exp Biol **172**(Pt 1): 345-354.

Korzellius, J., S. K. Naumann, M. A. Loza-Coll, J. S. Chan, D. Dutta, J. Oberheim, C. Glaesser, T. D. Southall, A. H. Brand, D. L. Jones and B. A. Edgar (2014). "Escargot maintains stemness and suppresses differentiation in Drosophila intestinal stem cell". EMBO J **33**(24): 2967-82

Kwon, D. H., K. S. Yoon, J. M. Clark and S. H. Lee (2010). "A point mutation in a glutamate-gated chloride channel confers abamectin resistance in the two-spotted spider mite, Tetranychus urticae Koch." Insect Mol Biol **19**(4): 583-591.

Li, J., F. He, Y. Yang, Y. Xiao, R. Peng, H. Yao, X. Li, J. Peng, H. Hong and K. Liu (2015). "Establishment and characterization of a novel cell line from midgut tissue of Helicoverpa armigera (Lepidoptera: Noctuidae)." In Vitro Cell Dev Biol Anim **51**(6): 562-571.

Liu, N and G. J. Scott (1996). "Genetic analysis of factors controlling high- level expression of cytochrome P450, CYP6D1, cytochrome b5, P450 reductase, and monooxygenase activities in LPR house flies, Musca domectica". Biochem Genet **34**(3-4): 133- 48

Loeb, M. J. (2010). "Factors affecting proliferation and differentiation of Lepidopteran midgut stem cells." Arch Insect Biochem Physiol **74**(1): 1-16.
Loeb, M. J., E. A. Clark, M. Blackburn, R. S. Hakim, K. Elsen and G. Smagghe (2003). "Stem cells from midguts of Lepidopteran larvae: clues to the regulation of stem cell fate." Arch Insect Biochem Physiol **53**(4): 186-198.

Loeb, M. J., N. Coronel, D. Natsukawa and M. Takeda (2004). "Implications for the functions of the four known midgut differentiation factors: An immunohistologic study of Heliothis virescens midgut." Arch Insect Biochem Physiol **56**(1): 7-20.

Loeb, M. J., E. A. Clark, M. Blackburn, R. S. Hakim, K. Elsen and G. Smagghe (2003). "Stem cells from midguts of Lepidopteran larvae clues to the regulation of fate". Arch Insect Biochem Physiol **53**(4): 186- 98.

Loeb, M. J. and H. Jaffe (2002). "Peptides that elicit midgut stem cell differentiation isolated from chymotryptic digests of hemolymph from Lymantria dispar pupae." Arch Insect Biochem Physiol **50**(2): 85-96.

Loeb, M. J., P. A. Martin, R. S. Hakim, S. Goto and M. Takeda (2001). "Regeneration of cultured midgut cells after exposure to sublethal doses of toxin from two strains of Bacillus thurigiensis". J Insect Physiol **47**(6): 599-606

Lynn, D. E. (1996). " Development and characterization of insect cell lines" Cytotechnology **20**: 3-11

Manjon, C., B. J. Troczka, M. Zaworra, K. Beadle, E. Randall, G. Hertlein, K. S. Singh, C. T. Zimmer, R. A. Homem, B. Lueke, R. Reid, L. Kor, M. Kohler, J. Benting, M. S. Williamson, T. G. E. Davies, L. M. Field, C. Bass and R. Nauen (2018). "Unravelling the molecular determinants of bee sensitivity to neonicotinoid insecticides". Curr Biol **28**(7): 1137- 1143.

Mermans, C., W. Dermauw, S. Geibel and T. Van Leeuwen (2017). "A G326E substitution in the glutamate-gated chloride channel 3 (GluCl3) of the two-spotted spider mite Tetranychus urticae abolishes the agonistic activity of macrocyclic lactones." Pest Manag Sci **73**(12): 2413-2418.

Michelli, C. A. and N. Perrimon (2006). "Evidence that stem cells reside in the adult Drosophila midgut epithlium". Nature **439**(7075): 475-9

Mounsey, K. E., J. A. Dent, D. C. Holt, J. McCarthy, B. J. Currie and S. F. Walton (2007). "Molecular characterisation of a pH-gated chloride channel from Sarcoptes scabiei." Invert Neurosci **7**(3): 149-156.

Narahashi, T., X. Zhao, T. Ikeda, V. L. Salgado and J. Z. Yeh (2010). "Glutamate-activated chloride channels: Unique fipronil targets present in insects but not in mammals." Pestic Biochem Physiol **97**(2): 149-152.

Njue, A. I., J. Hayashi, L. Kinne, X. P. Feng and R. K. Prichard (2004). "Mutations in the extracellular domains of glutamate-gated chloride channel alpha3 and beta subunits from

ivermectin-resistant Cooperia oncophora affect agonist sensitivity." J Neurochem **89**(5): 1137-1147.

Oppold, A. M. and Mueller, R (2017). "Epigenetic: A hidden target of insecticides." Adv Ins Physiol **53**: 313- 324.

Pearce, S. L., D. F. Clarke, P. D. East, S. Elfekih, K. H. J. Gordon, L. S. Jermiin, A. McGaughran, J. G. Oakeshott, A. Papanicolaou, O. P. Perera, R. V. Rane, S. Richards, W. T. Tay, T. K. Walsh, A. Anderson, C. J. Anderson, S. Asgari, P. G. Board, A. Bretschneider, P. M. Campbell, T. Chertemps, J. T. Christeller, C. W. Coppin, S. J. Downes, G. Duan, C. A. Farnsworth, R. T. Good, L. B. Han, Y. C. Han, K. Hatje, I. Horne, Y. P. Huang, D. S. T. Hughes, E. Jacquin-Joly, W. James, S. Jhangiani, M. Kollmar, S. S. Kuwar, S. Li, N. Y. Liu, M. T. Maibeche, J. R. Miller, N. Montagne, T. Perry, J. Qu, S. V. Song, G. G. Sutton, H. Vogel, B. P. Walenz, W. Xu, H. J. Zhang, Z. Zou, P. Batterham, O. R. Edwards, R. Feyereisen, R. A. Gibbs, D. G. Heckel, A. McGrath, C. Robin, S. E. Scherer, K. C. Worley and Y. D. Wu (2017). "Genomic innovations, transcriptional plasticity and gene loss underlying the evolution and divergence of two highly polyphagous and invasive Helicoverpa pest species." BMC Biol **15**(1): 63.

Perry. T. and P. Batterham (2018). "Harnessing model organisms to study insecticide resistance." Curr Opin Insect Sci **27**: 61-67

Press, B. and D. Di Grandi (2008). "Permeability for intestinal absorption: Caco-2 assay and related issues." Curr Drug Metab **9**(9): 893-900.

Samantsidis, G. R., A. O. O'Reilly, V. Douris and J. Vontas (2019). "Functional validation of target-site resistance mutations against sodium channel blocker insecticides (SCBIs) via molecular modeling and genome engineering in Drosophila." Insect Biochem Mol Biol **104**: 73-81.

Schneider, D. (2000). "Using Drosophila as a model insect." Nat Rev Genet **1**(3): 218-226.

Shaw, R.L., A. Kohlmaier, C. Polesello, C. Veelken, B. A. Edgar and N. Tapon (2010). "The Hippo pathway regulates intestinal stem cell proliferation during Drosophila adult midgut regeneration". Development **137:** 4147-4158.

Smagghe, G., C. L. Goodman and D. Stanley (2009). "Insect cell culture and applications to research and pest management". In Vitro Cell Dev Biol Anim **45**(3-4): 93-105

Srinivasan, B., A. R. Kolli, M. B. Esch, H. E. Abaci, M. L. Shuler and J. J. Hickman (2015). "TEER measurement techniques for in vitro barrier model systems." J Lab Autom **20**(2): 107-126.

Sun, H., E. C. Chow, S. Liu, Y. Du and K. S. Pang (2008). "The Caco-2 cell monolayer: usefulness and limitations." Expert Opin Drug Metab Toxicol **4**(4): 395-411.

Wang, X., R. Wang, Y. Yang, S. Wu, A. O. O'Reilly and Y. Wu (2016). "A point mutation in the glutamate-gated chloride channel of Plutella xylostella is associated with resistance to abamectin." Insect Mol Biol **25**(2): 116-125.

Wen, Z., L. Pan, M. R. Berenbaum and M. A. Schuler (2003). "Metabolism of linear and angular furanocoumarins by Papilio polyxenes CYP6B1 co-expressed with NADPH cytochrome P450 reductase." Insect Biochem Mol Biol **33**(9): 937-947.

Yanagihashi, Y., T. Usui, Y. Izumi, S. Yonemura, M. Sumida, S. Tsukita, T. Uemura and M. Furuse (2012). "Snakeskin, a membrane protein associated with smooth septate junctions, is required for intestinal barrier function in Drosophila." J Cell Sci **125**(Pt 8): 1980-1990.

6. Supplementary

Table S1: List of primers used in all the three projects

No	Primer name	Sequence (5'→ 3')	Experimental use
1	Hz_MESH_F	AGACTACCAGAGAGACATCCAT	PCR for markers
2	Hz_MESH_R	GGACGCTGACTACCGATACG	PCR for markers
3	Hz_Tsp2A_F	TCCAGCATCCAGCCGTTGATAA	PCR for markers
4	Hz_Tsp2A_R	CCGTGGAAGTAAGCGTTGCC	PCR for markers
5	Hz_Ssk_F	CTACCTCATATACACGCTGGTGC	PCR for markers
6	Hz_Ssk_R	CTGCCAAACCAACCTGTTTCTC	PCR for markers
7	Hz_EF1_F	CAAGGAGGGTAAGGCTGAAG	PCR for markers
8	Hz_EF1_R	ACGATGACCTGTGCTGTGAA	PCR for markers
9	Hz_zip_F	TGCCGCCAGGACTAAGACTA	PCR for markers
10	Hz_zip_R	TCACTCTGCTCCTGAGCTTG	PCR for markers
11	Hz_Eip75B_F	CCTCAACGGCGTGGTGAAA	PCR for markers
12	Hz_Eip75B_R	GAGTGGGTTGCGAGTAGGTG	PCR for markers
13	Hz_Lab_F	GCAGCATACCAGCCACCTTA	PCR for markers
14	Hz_Lab_R	TGTGTTTGAACGGCTCTGGA	PCR for markers
15	Hz_CREG_F	AATGAGGTGACGATGAGCC	PCR for markers
16	Hz_CREG_R	ATTCCGCTGTGTTCTCGTGT	PCR for markers
17	Hz_Syx1A_F	CGCAGTATTCACACAGGGGAT	PCR for markers
18	Hz_Syx1A_R	GATCTATCAGCTCGCCCCGT	PCR for markers
19	Hz_pros_F	ATCGTCTCGTAAGCACGGCA	PCR for markers
20	Hz_pros_R	GTCCGTTCGTCGTGAGAGTC	PCR for markers
21	HzOG207811_F	GTCCATCATTCCCGTCGTCA	PCR for markers
22	HzOG207811_R	CGACGAATAACCTGGGCTGT	PCR for markers
23	HzOG206246_F	GCCACAAGGACGGTAGTCAA	PCR for markers
24	HzOG206246_R	GGACGGTGTTCTCTCCCAAG	PCR for markers

25	Ha_Hz_Insc_F	GCTGAACAACCGAGACGAGA	PCR for markers
26	Ha_Hz_Insc_R	CACCAGTACAGTGATGTGCT	PCR for markers
27	Ha_Hz_Lrch_F	GGAGCGACATCTTCAGACGG	PCR for markers
28	Ha_Hz_Lrch_R	GTGGAATACAACGGTCGGGT	PCR for markers
29	Ha_Hz_Su_F	GCAGATGACCCAGTATCCCA	PCR for markers
30	Ha_Hz_Su_R	CATAGTCTCTGCTTCCACGTC	PCR for markers
31	Ha_Hz_Tk_F	AGCACCAATGGGCTTCATGG	PCR for markers
32	Ha_Hz_Tk_R	GTCCTTTTTGCCCCTCACAC	PCR for markers
33	T7 (addgene) forward	TAATACGACTCACTATAGGG	Colony PCR for gRNAs
34	T7 terminal (addgene) reverse	GCTAGTTATTGCTCAGCGG	
35	Dmel_GluCl_gRNA_F	CTTCGAAGGCCATCGATGTGTGGAC	dsDNA synthesis-gRNA construction
36	Dmel_GluCl_gRNA_R	AAACGTCCACACATCGATGGCCTTC	
37	Dmel_GluCl_generic_F	TCAGCATTAAAGAACCAGCGT	Screening of modified flies
38	Dmel_GluCl_generic_R	ATGCATAGTTCACCAGGGCG	
39	Dmel_GluCl_specific_R	CACGCCTGTCCAGACGTCGG	
40	EGFP_FP	ATGGTGAGCAAGGGCGAG	Cloning and screening
41	EGFP_RP	TTACTTGTACAGCTCGTCCATGC	

Table S2: 1:1:1 (*D. melanogaster*: *H. armigera*: *H. zea*) midgut cell type markers orthologues. *Dm*_FBgn: Flybase gene name, name: name of the *Drosophila* gene, *Ha*_og: *H. armigera* gene, annot: annotation name, *Hz*_og: *H. zea* gene name, mid. mean: mid mean of midgut genes expression of *H. armigera* in L2, L3 & L4 larval stages compared to carcass, Cell type: midgut cell types → ISC: intestinal stem cell, EC: enterocyte, EE: enteroendocrine cell

*Dm*_FBgn	name	*Ha*_og	annot	*Hz*_og	mid.mean	Cell type
FBgn0265434	Zip	HaOG211344	myosin heavy chain, non-muscle	HzOG211344	583,8	ISC
FBgn0000568	Eip75B	HaOG205019	ecdysone-inducible protein E75	HzOG205019	309,6	ISC
FBgn0002522	Lab	HaOG21676	homeotic protein labial-like	HzOG216768	196	EC
FBgn0025456	CREG	HaOG213019	protein CREG1	HzOG213019	138,1	EC
FBgn0024997	CG2681	HaOG205505	putative E3 ubiquitin-protein ligase SINAT1	HzOG205505	112,8	
FBgn0014018	Rel	HaOG206146	nuclear factor NF-kappa-B p110 subunit	HzOG206146	109,7	ISC
FBgn0003391	Shg	HaOG209732	DE-cadherin	HzOG209732	104,7	ISC
FBgn0010113	Hdc	HaOG207182	headcase protein	HzOG207182	82,5	ISC
FBgn0086347	Myo31DF	HaOG208687	myosin-IA	HzOG208687	69,4	EC
FBgn0004914	Hnf4	HaOG206928	hepatocyte nuclear factor 4-gamma	HzOG206928	65,3	EC
FBgn0259176	Bun	HaOG215895	protein bunched, class 2/F/G	HzOG215895	63,4	ISC
FBgn0004456	Mew	HaOG212624	integrin alpha-PS1	HzOG212624	59	ISC
FBgn0001235	Hth	HaOG207086	homeobox protein homothorax	HzOG207086	58,6	EC
FBgn0045852	Ham	HaOG217067	PR domain zinc finger protein 16-like	HzOG217067	48,9	EC
FBgn0004657	Mys	HaOG204948	integrin beta-PS	HzOG204948	47,5	ISC
FBgn0013343	Syx1A	HaOG212173	syntaxin-1A	HzOG212173	46,8	EE
FBgn0011674	Insc	HaOG213564	uncharacterized protein	HzOG213564	38,4	ISC
FBgn0262582	Cic	HaOG208209	uncharacterized protein	HzOG208209	34,3	ISC
FBgn0032633	Lrch	HaOG208026	leucine-rich repeat and calponin homology domain-containing protein 3	HzOG208026	19,8	ISC
FBgn0037976	Tk	HaOG215049	tachykinins-like	HzOG215049	19,6	EE

FBgn0031294	IA	HaOG212194	receptor-type tyrosine-protein phosphatase N2	HzOG212194	18,1	EE
FBgn0000251	Cad	HaOG204062	homeobox protein CDX-1-like	HzOG204062	14,8	EC
FBgn0015591	AstA	HaOG213960	helicostatins	HzOG213960	13,5	EE
FBgn0004837	Su(H)	HaOG213319	suppressor of hairless	HzOG213319	13,4	ISC
FBgn0037408	NPFR	HaOG202243	neuropeptide F receptor	HzOG202243	12,9	
FBgn0261930	Vnd	HaOG203257	homeobox protein XENK-2-like	HzOG203257	12,6	EC
FBgn0004648	Svr	HaOG213686	carboxypeptidase D-like	HzOG213686	12,4	EE
FBgn0032048	Dh31	HaOG201659	diuretic hormone class 2	HzOG201659	10,2	EE
FBgn0020912	Ptx1	HaOG205298	pituitary homeobox homolog Ptx1	HzOG205298	10,1	EC

>GluCl_I310T (1708 bp)
TGAAATTTAAGCAAACGAAAGCCAAAAGCTGCAAACGATACCTCTCTTATGACATCCTCCCGTACATTTTGAGTTT
GACACATTTTATATACCTTGTATACTCATAGGTGAATACAGTTGCCTCAAAGTCGATCTACTATTCAAGCGAGAAT
TCTCATATTACTTAATACAAATTTATATACCATGCTGTATGTTGGTCATTGTATCATGGGTATCATTCTGGCTGGA
TCAAGGAGCAGTACCGGCGCGAGTGTCACTGGGTAAGTACGCATTTTCAATTTGCCTCCTCAACGTGTCAACAAAA
TGTGTGTTATAATATCTACTACATTTTTGACTATTTTATAAACATAGCCCAACGTATAAGTATATAAAAAAAGATT
TGAAATCGTTGCCAGATATGTTCCTTTTTGCCATTTCTAAAATGACGGCTTAATAACAAGGAAATAATATTACCAT
CAATCAGCATTAAAGAACCAGCGTTATATTACACAAAAAATTATTTTCAGAAGTTCCAATAATACAAATAGAATAT
CTCTATTGATCTATCAAAAAACTTAACTTAAATCAATCTTCTTTGAAGATATTGTTTTCACCAGACGCTTTTTAAG
CTAATCGACGCACTTTACTTTAATTATAAAATAGTCAAGAAACAAAGTTAATATTTTGAAAAAGTAGTAGGTATTA
AATATACACTCCAACCTTACCAAATCTGATGCTAGTCCTTGGAGCCCGTCCTTCTTCATAGTCTAGAACACCAGTT
TGTTGGGCACTACTCCATTACCTCTTTTGCAGGTGTCACCACCCTGCTGACCATGGCCACCCAGACGTCGGGCATA
AACGCGTCCCTGCCGCCCGTTTCCTATACGAAGGCCACCGACGTCTGGACAGGCGTGTGTCTGACGTTCGTGTTCG
GGGCCCTGCTCGAGTTCGCCCTGGTGAACTATGCATCCCGATCAGGTTCGAATAAAGCTAGTAATTGAACTTTTAT
ATGCTTCTTAACCACGTATAAATGTTAATTAATCGATGGTGTTTATCTTTTTTCTGTTGTTTTATTGTACTGAGTG
ATATCGAATATACTATACGTACATATCTATAGTAACCACATATAAATGTCTACGCATACTGTACATACAACAACTC
TGAAACTTTGAAACTCAGAACCAACGTCACACTCTCAATATCTCACACACACACGAGTTACTCACTGTGGACCGTT
ATATCAGAACACTCACACACGCAGGACCGGCGTGGCTCACACAACAACAACAAGAACTACAACCAGTCTCGGGCTA
TATATCTAACGAATATCGAATGTCGAATATATCCATATAGAGTACACCCAGCGTACTTGTCTATATTTCCGAGCGA
AAGCCCAACGATTTAGCCGTAGTGTTTTTGATCGACTTTTTTCCCTTATTTACTTTTCACTTTGATATCTAACCAC
AAAATGGGTTCATCGTGTGTATCAAACTAATCCAACTTTTTGTTTTACTCTCTTATTTCATTGTGCGCCCACCATT
CATCGACATGCATACGAACATACACATGCACAATCCGCAAACTACATACCCACACCCAAACGCACACACCAATACC
AATGCCAATACCAATACCAAAACCAATACACACGAACCACGAACTTTAAACGCGTTTGAAAAAACACATAAACCGA
AAATTGTAAACAAATTGGTCGAATTTCCTGTCGAAT

Supplementary figure 1*:* Sequence of donor plasmid for generation of ATC → ACC substitution, I310T mutation, via CRISPR/ Cas9 system in *GluCl* gene of *D. melanogaster*. Highlighting in red the under study alteration and in blue the diagnostic synonymous alterations. The size of this plasmid is 1708 bp.